Semi-Annual Status Report

for the Period

January 1, 1967 - June 30, 1967

AN EXPERIMENTAL INVESTIGATION OF
RADIATION EFFECTS IN SEMICONDUCTORS

National Aeronautics and Space Administration

Washington, D. C.

Research Grant No. NsG 22862

W. Dale Compton

Principal Investigator

Coordinated Science Laboratory
University of Illinois
Urbana, Illinois 61801

Introduction

Irradiation of semiconductors with high-energy radiation, e.g., neutrons, gamma rays, and fast electrons, introduces vacancies and interstitials that diffuse through the lattice and combine with impurities or other defects. The Si-A center is created by the association of an interstitial oxygen atom with a lattice vacancy. The Si-E center is created by the association of a lattice vacancy with a substitutional phosphorous impurity. The defects that are formed from the primary displacements depend upon the oxygen content of the crystal, the concentration and type of dopant, the temperature of the irradiation, and the subsequent temperature of annealing after the irradiation. Work carried out under this grant is intended to provide information about the nature of these defects. It is particularly important to determine the microscopic nature of the defect and the nature of the interaction of the defect with the lattice, particularly the phonon-electron interaction.

A new technique has been developed for studying these defects involving an analysis of the recombination luminescence resulting from electron-hole recombination at the defect. Past studies have been carried out of the effects of irradiation upon the conduction mechanism of highly-doped semiconductors. This has led to an interpretation that the mechanism of conduction involves impurity bands whose population and width can be varied by the radiation. In order to establish the validity of this interpretation, it is necessary to determine directly the nature of the impurity bands. This is being attempted by a technique involving the tunneling between a semiconductor and a superconductor.

Recombination Luminescence

Extensive measurements of the recombination luminescence of samples of n- and p-type silicon have been made at 77°K and 6°K. Both Czochralski and float-zone grown material have been used in the study. Irradiations were made with both CO^{60} gamma rays and with fast neutrons. This work forms the basis of the Ph.D. thesis of Mr. Robert Spry.

Although it was anticipated that this thesis would be completed during the last six months, the extensive analysis of the data that were required have delayed it somewhat. It is now nearing completion and will be submitted for final approval in the next month.

As a result of the extensive nature of the thesis, a detailed discussion of the results will not be included. A couple of points, not specifically reported in previous status reports, are of sufficient interest that they will be mentioned here. Figures 1 and 2 present spectral data taken at 6°K on both pulled and float-zone grown silicon. Figure 1 gives the results of five measurements on 100 ohm-cm n-type material following irradiation with about 10^8 roentgens of CO^{60} gamma rays. Several features of the curves are clearly reproduced in each of these measurements. Of particular interest, however, are those features that are not the same. The low energy pattern, extending between 0.65 and 0.80 eV, is initially low immediately after irradiation, grows substantially for several days and then gradually anneals when the sample is maintained at room temperature for the number of days indicated. All of these measurements were made relative to the nearly constant height of the high-energy peak in

the spectrum at 0.9707 eV. In addition, some of the detailed structure annealed in the low energy portion. Particularly noticeable is the small bump on the high-energy side of the 0.7905 eV peak that disappeared after a short time. Figure 2 presents some comparable data on float-zone grown material. There is a distinct change in the background level of the luminescence following the room temperature anneal of several days.

These observations point up the amount of detail that can be obtained by measurements of this type. Present activities include a complete redesign of the experimental equipment that will allow for a greater spectral resolution of the luminescence data and with the possibility of applying a uniaxial stress to the sample at low temperatures. The liquid helium dewar has been modified. A new detector system, utilizing a high sensitivity PbS detector and as an alternate an InSb detector, has been provided. Auxiliary equipment to allow direct coupling of the data system to the CDC-1604 computer has been designed and is being fabricated.

Preliminary measurements of the recombination luminescence of irradiated germanium are being initiated with the previously-used equipment. No results are yet available. It is anticipated that substantial data will be acquired during the next few months.

Tunneling Conductance Measurements on p-Type Silicon

The electronic properties of heavily-doped semiconductors, which are of particular importance for device applications, are not completely understood, even for germanium and silicon. Measurements of electrical

resistivity as a function of temperature for donor or acceptor concentra-
tions approaching those required for degeneracy[1] (i.e., the Fermi level
lies at least a distance kT into the conduction or valence band) indicate
that low-temperature electrical conduction occurs by motion of carriers
in concentration-broadened levels (in the forbidden gap) derived from
the original donor or acceptor states. The conduction processes can be
separated into two types: "hopping" processes, requiring thermal activa-
tion and some degree of compensation, and "impurity-band" conduction,
resulting when overlap of impurity wavefunctions and screening become
important enough to cause a transition from localized impurity states to
delocalized or traveling wave states, and hence conduction with no thermal
activation required. The electrical measurements suggest that a split-off,
narrow impurity band may exist in the gap close to the conduction- (or
valence-) band edge, and which merges with the conduction (valence) band
as the concentration increases to that required for complete degeneracy.
The role of the impurity centers for further increases in concentration,
apart from that of scattering the conduction (valence) traveling-wave
states, is not known. Some theoretical arguments[2] suggest that altera-
tions in the electron density of states in the region between the band
edge and the Fermi level, in the position of the Fermi level as a func-
tion of concentration and temperature, and in the energy-wave-vector
dispersion relation may result from interaction between the carriers and
the impurities.

The feasibility of directly measuring some of these properties in
the region of high doping, namely the density of states and the Fermi-

level position with respect to the band edge, by means of a metal-semiconductor tunneling experiment, has been investigated. The semiconductor chosen was silicon containing boron, for which degeneracy occurs at a doping of about 10^{19} cm^{-3}. The tunneling configuration is best described as a metal-semiconductor contact, or Schottky barrier diode.[3,4] The tunneling contact is formed on a freshly-cleaved [111] silicon plane by application of a clean point of indium wire. The indium flows under an applied force to form a mechanically-firm cold weld to the silicon which withstands temperature cycling to 4°K. Contact areas have been varied from about 0.5 mm^2 to about 0.01 mm^2. The contacts are formed in the air, so that the surfaces are covered with adsorbed gases. The thermal oxidation rate of silicon at room temperature is sufficiently small[5] that a negligible thickness of oxide develops. Thus, the contacts continue to behave electrically as Schottky barriers.

The theory of tunneling in such a metal-semiconductor contact has recently been described. A potential barrier (the Schottky barrier) is formed in the semiconductor under the contact by the transfer of carriers from the region of the bulk near the surface to surface states.[6,7] The solution of Poisson's equation assuming the total depletion of the material near the surface gives a parabolic potential variation proceeding inward from the surface.[3,4]

For the case of p-type silicon, the energy of the valence-band edge relative to its position in the bulk, as a function of the distance z from the surface is given by

$$E_V(z) = -(2\pi^2 e N_A/\varepsilon_0)(z-d)^2 \tag{1}$$

in which

$$d = (B+E_F-V)^{1/2}/(2\pi N e^2/\varepsilon_0)^{1/2} \tag{2}$$

and the symbols have the following meaning: N_A is the concentration of acceptors in cm^{-3}, ε_0 is the static dielectric constant (11.8 for silicon), e is the electron charge, E_F is the position of the Fermi level in the valence band, again measured down from the (bulk) valence-band edge, V is the applied bias voltage across the deflection layer, with sign such that positive V subtracts from the total energy variation, which is $|E_V(0)|$, and B is the energy of the valence-band edge at the surface measured down from the Fermi level.

The process of interest is the tunneling of carriers into the silicon bulk, i.e., holes located in energy between the bulk valence-band edge and Fermi energy, out to the metal. For a positive hole having energy u in the valence band measured from the bulk valence-band edge, $-E_V(z)-u$ represents a potential barrier, which must be tunneled through. The transmission factor, in the WKB approximation, for this barrier, i.e., $T = \exp(-2\int_0^{z(u)}|K|dz)$, in which $|K|^2 = (2m^*/\hbar)[-E_V(z)-u]$, can be calculated exactly,[4] giving

$$T = \exp\{-(R_0 R_u/E_0)+(u/E_0)\log[(R_0+R_u)/\sqrt{u}]\} \tag{3}$$

in which

$$E_0^2 = \hbar^2 \pi e^2 N_A/m^* \varepsilon_0 \tag{4}$$

and the symbols $R_u = \sqrt{(B+E_F-V-u)}$ and $R_o = \sqrt{(B+E_F-V)}$ are used. Here, m^* is the effective mass of the tunneling hole. An important feature of Schottky barrier tunneling, namely the bias-voltage dependence of the transmission factor, is evident in this expression. For $u = 0$, and $V << B$ one finds approximately

$$T = \exp[-(B+E_F0/E_o]\exp(V/E_o) \qquad (5)$$

showing the exponential increase of T for forward bias V. Also, the bias-independent factor of the transmission factor $\exp[-(B+E_F)/E_o]$ depends on the concentration N_A through the parameter E_o.

Figures 3 and 4 show measured liquid-helium temperature differential conductance di/dV curves for p-type silicon samples containing 1.2×10^{19} cm^{-3} and 4.4×10^{19} cm^{-3} boron. The straight-line behavior observed for positive bias V in these semilogarithmic plots is identified with the exponential increase of the transmission factor expected from Eq. 5. Further, the slopes of log di/dV vs V determine the parameter E_o, giving 42 meV and 69 meV for the 1.2×10^{19} -cm^{-3} and 4.4×10^{19} -cm^{-3} samples. These values are close to values of E_o calculated from the definition (4), if one assumes an effective mass $m^* = 0.23$, close to the measured light hole mass of 0.16 for silicon. The bias voltage at which the minimum in conductance di/dV occurs is expected from the work of Conley, et al.[4] to measure E_F, the Fermi level as measured from the bulk valence-band edge. As a rough check of the concentration dependence of the transmission factor, the value of di/dV at the minimum, put on a unit-contact-area basis by visually estimating the contact areas under nominal

magnification, has been compared for samples of varying acceptor concentration N_A. From Eqs. 4 and 5, the logarithm of the transmission factor T should vary linearly with the inverse square root of the acceptor concentration N_A. This behavior is observed, and is shown in Fig. 5. From the slope of this plot, and the value of E_o, 69 meV determined from the slope of the log di/dV-vs-V plot in Fig. 4, one gets an estimate for the barrier height B of 0.29 volt. This approximate value is close enough to the literature value[7] B = 0.3, E_o = 0.33 eV for silicon to give one some confidence in the Schottky barrier model.

Structure at zero bias corresponding to the superconducting energy gap in the indium appears when the samples are cooled below 3.41°K, the critical temperature. An example of this is shown in Fig. 6, a tracing of the direct x-y recorder plot for the 4.4×10^{19} -cm^{-3} sample at a temperature near 2°K. This structure can be extinguished by an applied magnetic field, revealing no other kind of zero-bias anomaly. The structure in Fig. 6 at about 60 mV is genuine and is shown in greater detail in Fig. 7. It is tentatively identified as a polaron effect by its proximity to the k = 0 phonon of energy 63.1 millivolts and its similarity to polaron anomalies in other materials identified by Conley and Mahan.[4]

The degree to which this type of experiment can be used to deduce the density-of-states function in the vicinity of the band edge of semiconductors is not clear at present.[4,8,9] The rise of di/dV to negative bias in Figs. 3 and 4 is thought certainly to reflect in some way the valence density of states, but the observed rise is not proportional to

the square root of the bias measured from the position of the di/dV minimum as would be expected if di/dV were proportional to the density of states in the simplest band picture. The observed rise of di/dV for reverse bias is nearly linear in voltage for samples shown in Figs. 3 and 4.

It is thought from the preliminary work reported that the method does hold considerable promise for studying the electronic properties of p-type silicon for concentrations very close to and exceeding that required for degeneracy.

Minority Carrier Lifetimes in Irradiated Silicon

No work is presently underway in this area. A manuscript based upon the Ph.D. thesis of Dr. Ralph Hewes has been prepared and submitted to the Journal of Applied Physics. A copy of this manuscript is attached to this report.

Personnel

Dr. E. L. Wolf, Mr. Robert Spry, Mr. Colin Jones, and Mr. Eric Johnson were employed for all of the time during the past six months.

References

1. See for instance E. A. Davis and W. Dale Compton, Phys. Rev. 140, A2183 (1965) and references cited in this paper.

2. The Electronic Theory of Heavily Doped Semiconductors, by V. L. Bonch-Bruevich, American Elswier (1966). Also B. I. Halperin and Melvin Lex, Phys. Rev. 148, 722 (1966).

3. J. W. Conley, C. B. Duke, G. D. Mahan and J. J. Tiemann, Phys. Rev. 150, 466 (1966).

4. J. W. Conley and G. D. Mahan, "Tunneling Spectroscopy in GaAs," Phys. Rev. (to be published).

5. B. A. Deal and A. S. Grove, J. Appl. Phys. 36, 3770 (1965).

6. Volker Heine, Phys. Rev. 138, A1689 (1965).

7. C. A. Mead and W. G. Spitzer, Phys. Rev. Letters 10, 471 (1963).

8. W. A. Harrison, Phys. Rev. 123, 85 (1961).
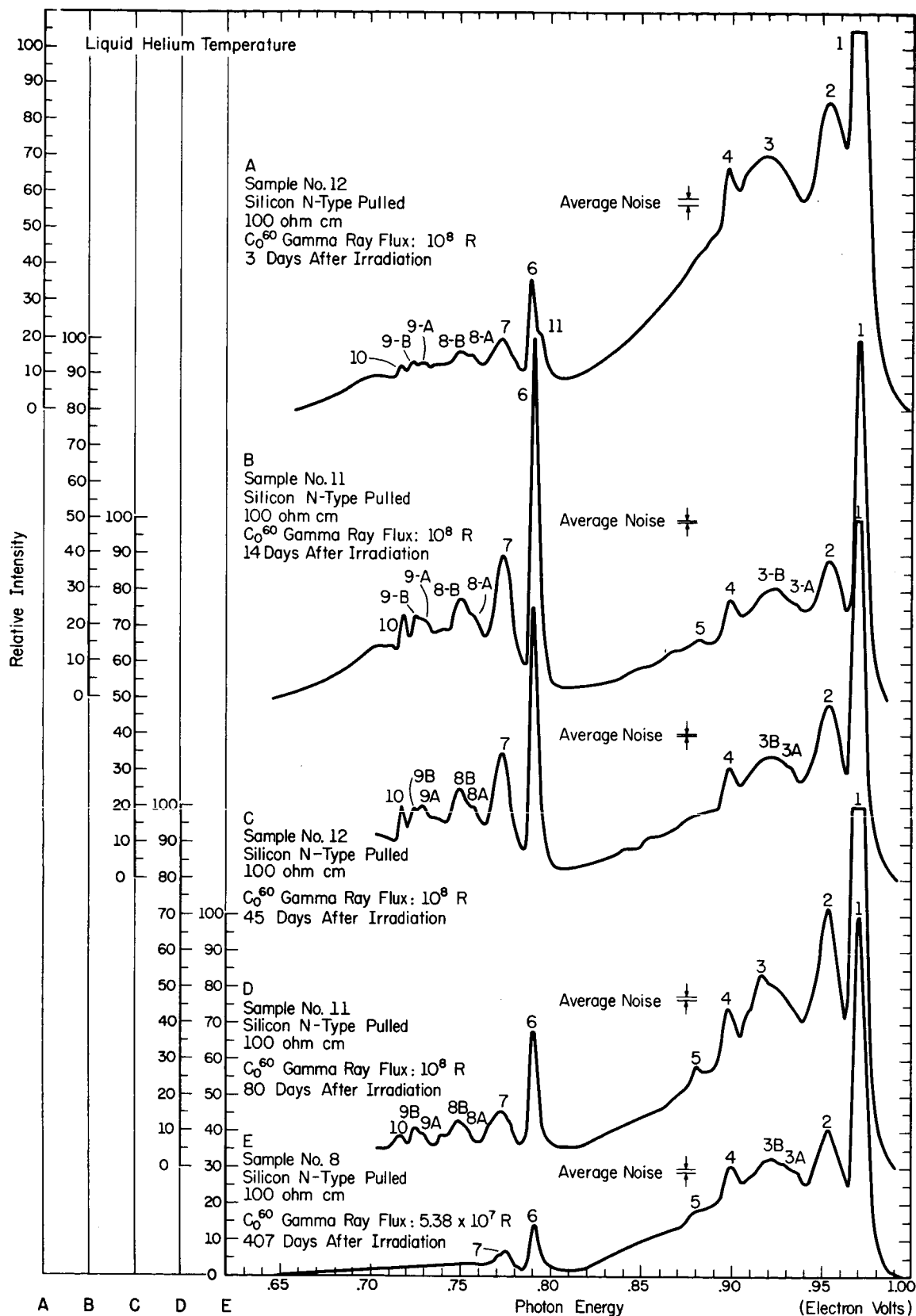
9. R. T. Shuey, Phys. Rev. 137, A1268 (1965).

Figure 1.   Recombination luminescence in gamma ray
            irradiated n-type Czochralski grown
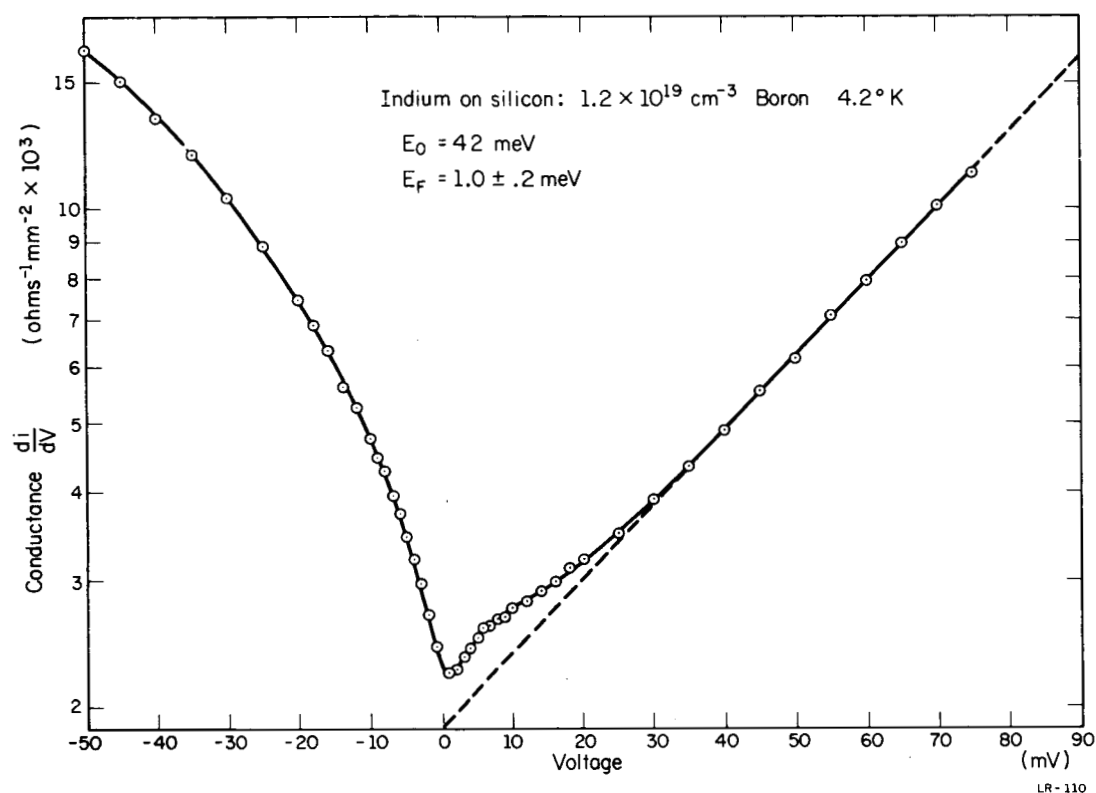   silicon.

Figure 2.   Recombination luminescence in irradiated
n-type float-zone grown silicon.

Indium on silicon: 1.2×10^{19} cm^{-3} Boron 4.2°K

$E_O = 42$ meV

$E_F = 1.0 \pm .2$ meV

Conductance $\frac{di}{dV}$ (ohms^{-1}mm^{-2} × 10^3)

Voltage (mV)

LR-110

Figure 3. Tunneling conductance for indium – p-type silicon contact at 4.2°K. The silicon contains 1.2×10^{19} cm^{-3} boron. The value E_O is derived from the slope for positive bias V.
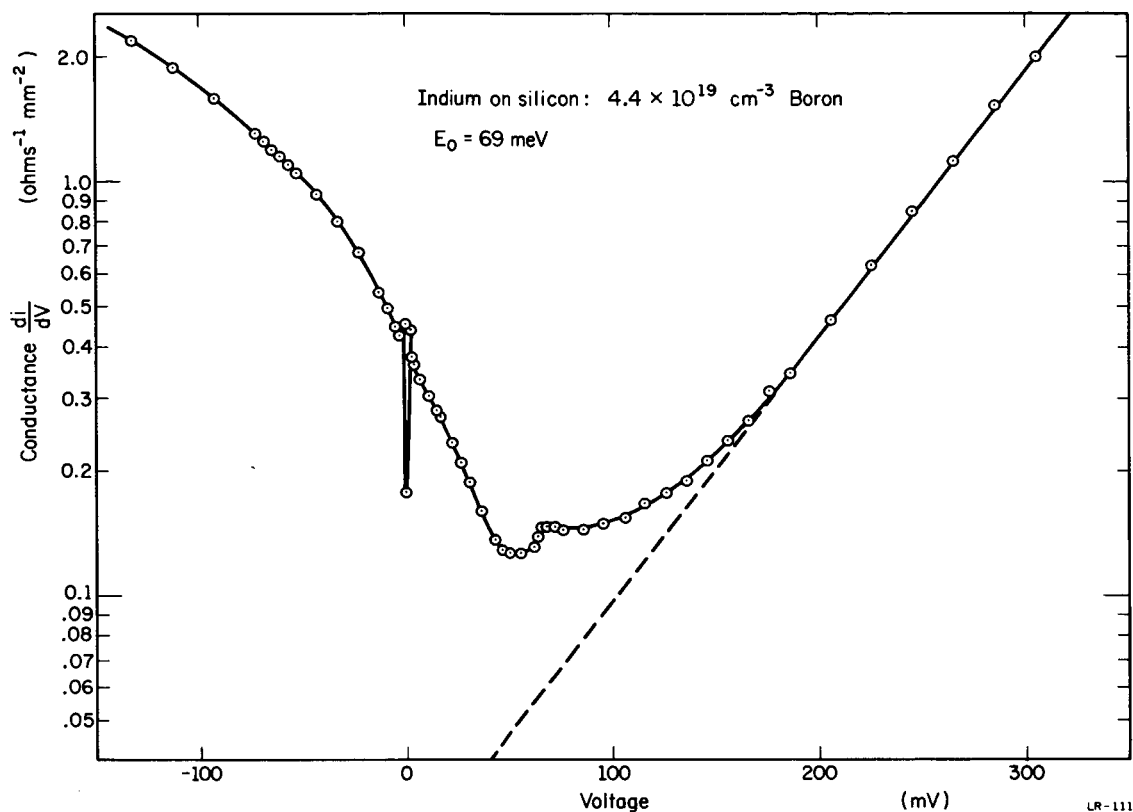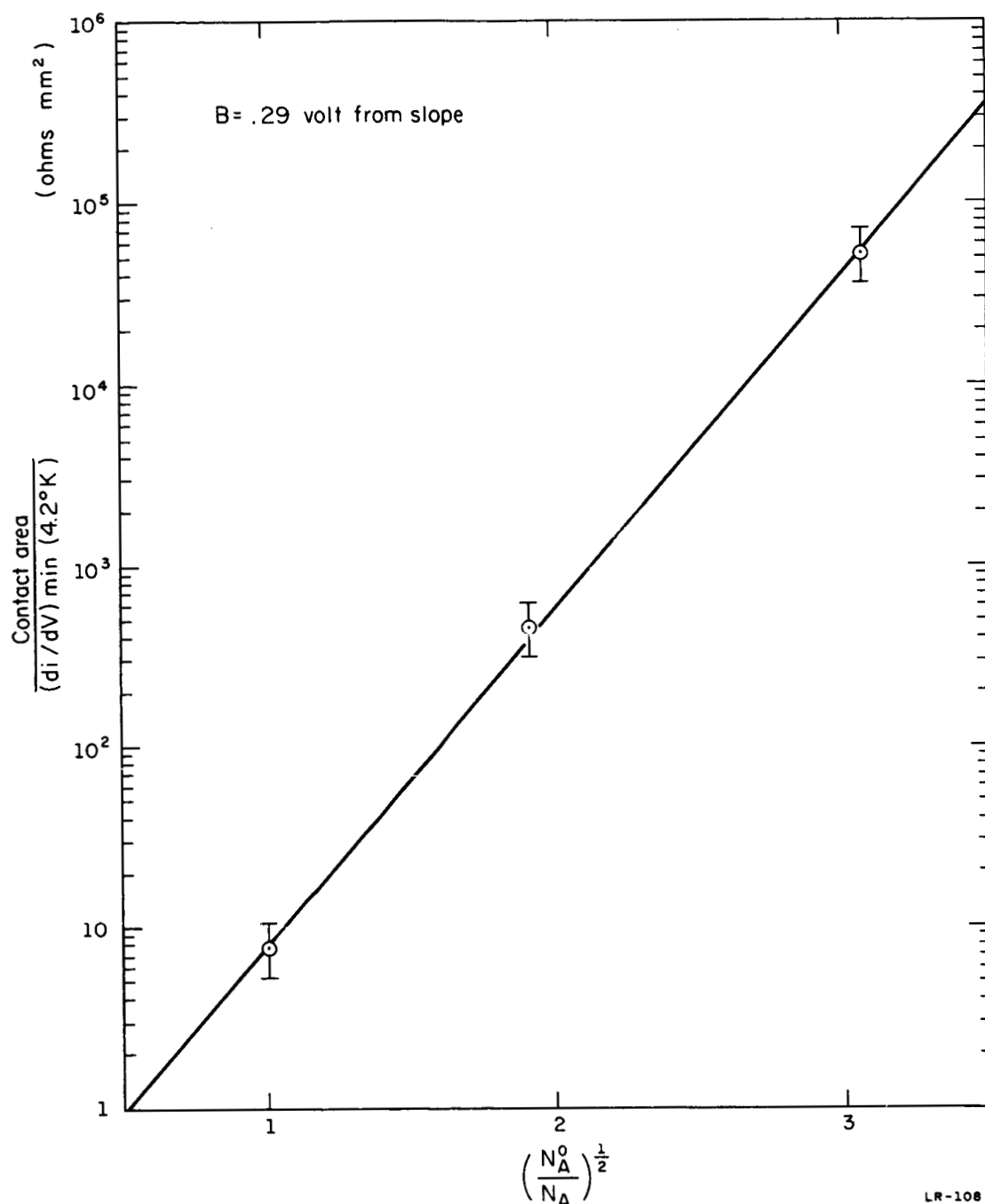
Figure 4. Tunneling conductance for indium on
silicon containing 4.4×10^{19} cm^{-3}
boron at a temperature near 2°K. The
position of the di/dV minimum is
complicated by the additional structure
at 64 meV (see Fig. 7) but one can
estimate $E_F = 50$ millieV.

Figure 5. The reciprocal of the tunneling conductance per unit contact area at 4.2°K and bias voltage equal to the Fermi level E_F is plotted against the inverse square root of the acceptor concentration N_A normalized to $N_A^\circ = 4.4 \times 10^{19}$ cm^{-3}. The three data points shown from left to right correspond to $N_A = 4.4 \times 10^{19}$ cm^{-3} and 4.7×10^{18} cm^{-3}, 1.2×10^{19} cm^{-3} and 4.7×10^{18} cm^{-3}, respectively. A straight line as observed is expected from Eqs. (4) and (5) if the effective mass, m^*, is independent of concentration N_A. The value $B = 0.29$ eV is obtained from the slope and the value $E_o = 69$ millieV measured on the 4.4×10^{19} cm^{-3} contacts.
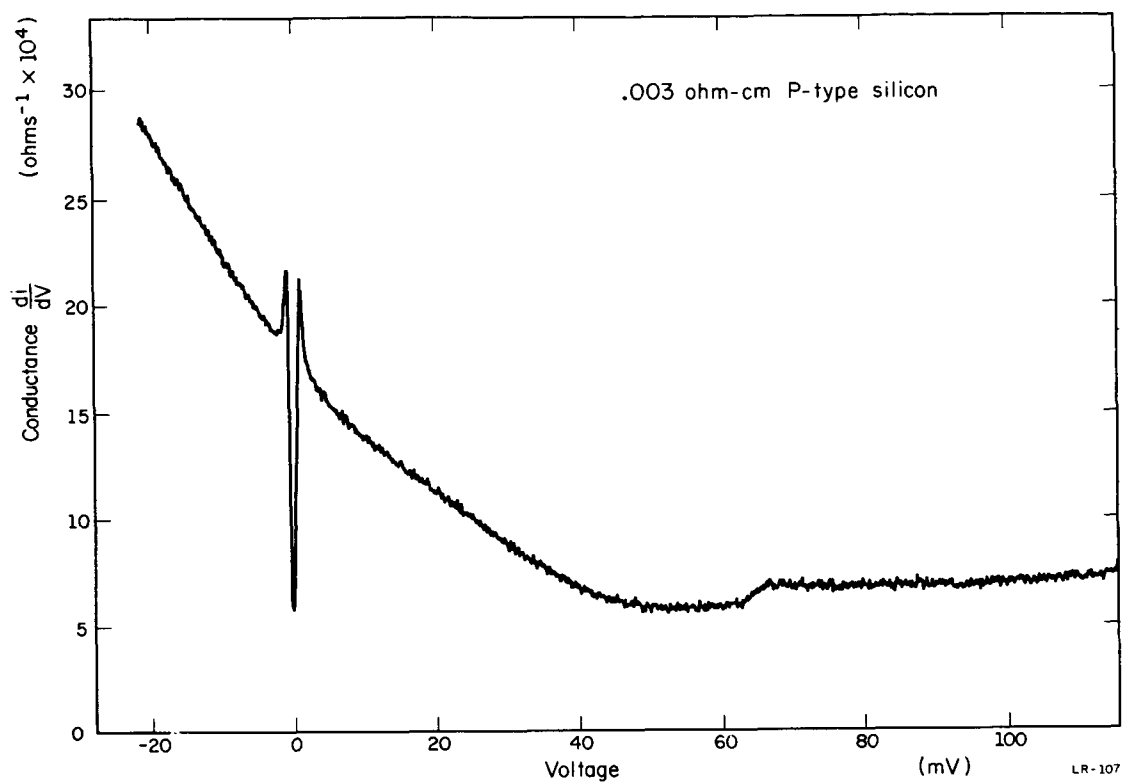
Figure 6. Differential conductance at pumped
helium temperature for $N_A = 4.4 \times 10^{19}$ cm^{-3}
sample, showing superconducting structure
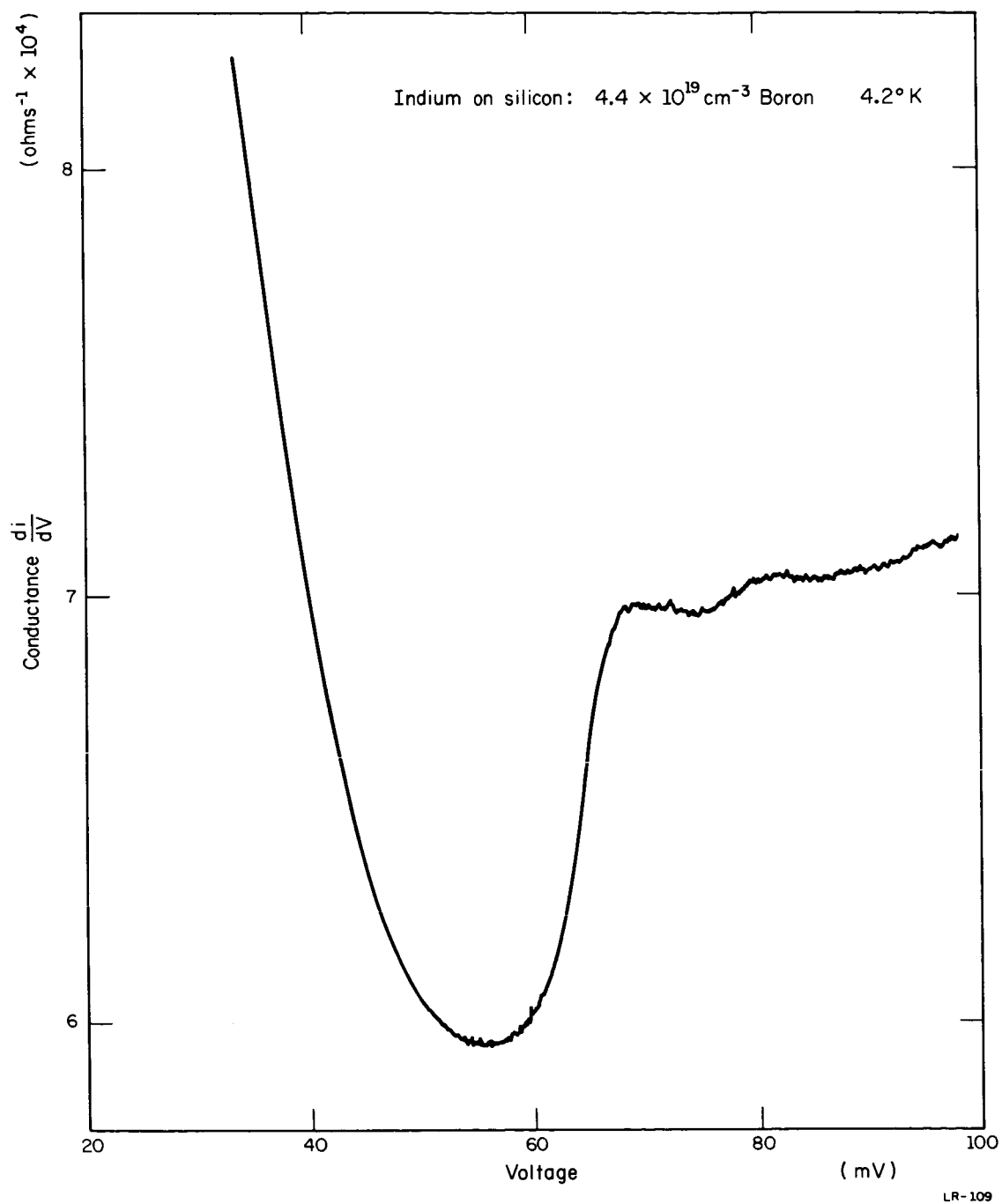at zero bias and anomalous structure at
64 meV.

Figure 7. Detail of anomalous structure in di/dV near
64 meV in 4.4 x 10^{19} cm^{-3} sample.

Recombination Lifetimes in Gamma-Irradiated Silicon[*†]

Ralph A. Hewes[‡]
Department of Physics, University of Illinois, Urbana, Illinois

Abstract

Photoconductivity decay measurements on a wide variety of silicon crystals (boron and phosphorus doped, Czochralski and float zone grown, $20 \leq \rho \leq 200$ ohm-cm) irradiated with Co^{60} gamma rays indicate that a separate system of levels controls the radiation induced lifetime in n- and p-type specimens. In n-type material the introduction rates for two recombination active defects (the A center and a deeper level) were seen to be nearly independent of oxygen and donor concentrations in the range en-

encountered in the experiment, while the introduction rate of a second deep level, the E center (vacancy-phosphorus pair) was seen to be inhibited by the presence of oxygen, and to increase with increasing donor concentrations. The behavior of the lifetime was studied after the samples were annealed, and it was found that a shallow level 0.23 eV from the conduction band edge was introduced. Hole capture cross sections for the two deep levels were obtained from Hall and lifetime measurements. In p-type material recombination levels at E_v + 0.18 eV and E_c - 0.3 eV were introduced by irradiation. The introduction rate of the level nearest the conduction band was strongly inhibited by the presence of oxygen and dominated the lifetime only in float zone material. Low temperature annealing was seen to occur in the defects having levels at E_c - 0.3 eV with the subsequent creation of defects with levels at E_v + 0.18 eV in some materials. In other materials a second type of defects with levels at E_c - 0.3 eV were created, while in some materials a simple annealing with no creation of new defects was found.

I. INTRODUCTION

Various experiments on electron- and gamma-irradiated silicon have yielded much information about the defects created by irradiation. Hall measurements[1-11] have been used to locate the positions of the energy levels of defects that can remove carriers from the conduction and valence bands (provided the levels lie in the same half of the forbidden gap as the Fermi level). Electron spin resonance experiments have been useful in determining the symmetry of some of these defects, with the result that models have been proposed for their structure.[12-14]

Lifetime measurements which have the potential of revealing the position of recombination levels which lie in the opposite half of the gap from the Fermi level, as well as those in the same half, have been used in many experiments,[11,15-21] but there is little agreement in the results. There are many techniques to measure the lifetime,[22] and in materials with large amounts of defects, possibly as many lifetimes as techniques, since some methods are dependent upon surface or junction effects to a great degree, and others more sensitive to trapping effects. Previous experiments have usually only investigated a small range of donor/acceptor and oxygen concentrations, and few measurements have used the same technique, so that a large amount of uncertainty exists about the effects of the above mentioned impurities (or of other impurities, such as chlorine[23]) upon the radiation induced recombination levels in silicon.

This experiment therefore used samples encompassing a relatively wide range of resistivity, both boron and phosphorus doped, with both

Czochralski (pulled) and floating zone grown (FZ) crystals, to determine

the effects of cobalt 60 gamma rays upon the lifetime as measured by the

photoconducitvity decay method. Of particular interest were the recom-

bination level positions, and the dependence of the radiation induced

lifetime upon the boron, phosphorus, and oxygen concentrations, and the

annealing behavior of the recombination centers.

In n-type material, where previous investigations had indicated

that the recombination levels were due to A centers[24] (substitutional

oxygen with an energy level 0.17 eV below the conduction band edge) and

E centers (phosphorus atom with a vacancy as a nearest neighbor, the

energy level 0.47 eV below the conduction band edge), Hall effect measure-

ments were made to determine the level positions independently, as well

as to obtain the defect introduction rates for use in the determination

of the capture cross sections of the defects for holes.

II. THEORETICAL BACKGROUND

Recombination of electrons and holes through a single set of

monovalent defects was first treated by Hall,[25] and Shockley and Read,[26]

who obtained the following solution for the lifetime, valid for steady-

state conditions and small excess carrier densities:

$$\tau = \tau_{po} \frac{(n_o + n_1)}{n_o + p_o} + \tau_{no} \frac{(p_o + p_1)}{n_o + p_o} \tag{1}$$

where $\tau_{po}^{-1} = \sigma_p N v_p$ = lifetime of holes in highly n-type material, τ_{no}^{-1} =

$N v_n \sigma_n$ = lifetime of electrons in highly p-type material, N is the concen-

tration of recombination centers, v_p and v_n are the hole and electron

thermal velocities, respectively, σ_p and σ_n are the capture cross sections of the recombination center for holes and electrons, n_0 and p_0 are the thermal equilibrium concentrations of free electrons and holes, and n_1 and p_1 are usually defined as the thermal equilibrium concentrations of electrons and holes when the Fermi level lies at the recombination center energy level ($n_1 = N_c \exp[(E_r - E_c)/kT]$, $p_1 = N_v \exp[(E_v - E_r)/kT]$, N_c and N_v are the effective densities of states in the conduction and valence bands, and E_r, E_v, and E_c are the energy levels of the recombination center, the energy levels of the valence and conductor band edges, respectively).

It should be pointed out that the foregoing definition of n_1 and p_1 does not take into account the fact that the (electron) occupied state of the recombination center contains only one more electron than the unoccupied state. Because of spin degeneracy, the electron that is added to fill the level is assumed to go into an orbital which may or may not already contain another electron. If the orbital contains another electron, then the level can be filled in only one way (spin opposite to that of the other electron), but can be emptied in two ways (losing either a spin-up or spin-down electron) so that the ratio of the degeneracies of the full to the empty level is 2. Likewise, if the orbital does not contain an electron, it can be filled in two ways but emptied only in one, so that the degeneracy ratio, ω, is now 1/2. Thus, a factor of ω should be included in the definition of n_1. If the hole formalism is employed in the foregoing argument, it can be shown that a factor of $1/\omega$ should be used in the definition of p_1.

Sandiford,[27] and Wertheim[28] showed that under conditions of small recombination center concentrations, the Shockley-Read (SR) result

will be valid for transient conditions such as are found in photoconduc-
tivity decay experiments. Wertheim also showed that for small enough
defect concentrations the net lifetime, τ, in the presence of 2 sets of
monovalent defects will be given by

$$\tau^{-1} = \sum_{i=1}^{j} \tau_i^{-1} \tag{2}$$

Where the lifetime τ_i is the SR lifetime for the ith set of defects.
The equation most probably applies for $j > 2$, provided none of the centers
act as traps for an appreciable fraction of the minority carriers.
Wertheim also considered the case of trapping, by setting σ_p or σ_n of one
of the two levels to zero, and obtained the result that Eq. (2) does not
hold. This subject has recently been extensively treated by Streetman.[29]
Nomura and Blakemore[30] have given a criterion for the concentration of
recombination centers for which the SR equations are valid. Shockley[31]
has shown that the surface recombination is describable as a term in
Eq. (2), provided only the fundamental surface decay mode is present.

Sah and Shockley[32] have treated the case of multilevel defects,
and found that the steady state lifetime will be given by

$$\tau^{-1} = \sum_{s=1}^{m} (N_s + N_{s+1})(N \tau_s)^{-1} \tag{3}$$

in the case of small excess carrier densities. The quantity N_s/N is the
fraction of defects occupied by s electrons, m is the maximum number of
electrons that are bound to the defect, and τ_s is the SR lifetime for a
monovalent defect having an energy level at E_s. N_s/N is given by

$$\frac{N_s}{N} = \frac{\overset{s}{\underset{k=0}{\pi}} \left(\frac{p_k}{p_0} = \frac{n_o}{n_k} \right)}{\overset{m}{\underset{s=0}{\Sigma}} \overset{s}{\underset{k=0}{\pi}} \frac{p_k}{p_0}} \quad (4)$$

where p_k is the quantity p_1 corresponding to the kth energy level, and when $k = 0$, $p_1 = p_{\hat{o}}$, the equilibrium hole concentration. From Eq. (3) and (4) we see that recombination through multilevel defects causes the lifetime to behave much the same as the lifetime due to separate sets of monovalent defects, with the effective concentrations of the defects dependent on the Fermi level position.

III. PROCEDURE

Lifetimes (actually half-decay times) of excess carriers were measured by the photoconductivity decay method. A spark discharge lamp, similar to the one used by Swank,[33] with a half decay time of less than 0.6 microseconds was used to create electron-hole pairs. The light was filtered by silicon filters varying in thickness from 1.5 mm to 7.5 mm, to insure uniform penetration of the exciting light. The 1.5 mm filter was used only when the lifetimes obtained with its use did not differ from those obtained with a much thicker filter, indicating that injection level effects[25] were not present. This was usually the case for the lower resistivity samples.

The samples were connected in series with a current-limiting resistor and a battery, and the transient portion of the sample voltage was amplified by a Tektronix type 1121 amplifier before being passed into

a Tektronix type 535A oscilloscope, using Tektronix type L or 1A1 vertical plug-in units. The sweep-delay feature of the type 535A was used to prevent display of at least the first half-decay of the signal, in order to minimize the effects of higher order modes of surface decay than the fundamental and the effect of the finite decay time of the light pulse. The oscilloscope trace was photographed with a Polaroid camera and the photographs of the traces were measured and plotted on semilog paper to obtain the lifetime. Several different sweep rates were used on each photograph so that the zero signal level could be determined.

Discs 5 mm in thickness were cut from cylindical boules. Rectangular parallelopipeds with dimensions typically 5 x 5 x 20 mm were cut from the discs. Some samples were seen to have large lifetime or resistivity variations along the sample length, which for the above prepared samples was a boule diameter. New samples of these materials were then cut with the sample length along the boule axis. No significant lifetime or resistivity variations were seen in the samples thus cut. At least two of the larger faces were polished to reduce reflection losses, and the other faces were ground. The effective surface recombination lifetimes (defined as the reciprocal of the carrier decay rate due to diffusion into surface recombination centers) were found to be very large. The electrical contacts were made by ultrasonically soldering indium to the samples, and the contacts were found to be ohmic in the temperature region where trapping did not prevent measurement of the lifetime. Electroless nickel plated contacts were used on some of the B and H samples.

Each sample was given a code letter and number, and its pre-irradiation characteristics were measured, and are listed in Table 1.

The letter designates the boule from which the sample was cut, and the number distinguishes between samples cut from the same boule. The lifetime was measured as a function of position along the sample length, and in those samples where significant variations were found, a region of nearly constant lifetime was selected for use during measurements. Voltages were chosen such that the excess carrier pulse did not drift out of this region.

The samples were glued onto copper sample mounts with G.E. #7031 insulating varnish, with layers of $\frac{1}{2}$ mil mylar between the sample and the mount, and between the sample and the copper-constantan thermocouple. The samples were mounted on the bottom of a vacuum dewar, but separated from the coolant reservior by a heater imbedded in a copper block. The temperature was varied by changing the power dissipated in the heater. A cooling mixture was placed in the dewar for reaching temperatures below room temperature.

The lifetime samples were irradiated at the U.S. Naval Research Laboratory in Washington, D. C., at approximately room temperature. The exposure rate was approximately 2×10^6 roentgens per hour. The irradiations histories of the samples are given in Table 2.

Post-irradiation lifetime measurements were made from low to high temperature. On the first sample of each resistivity to be measured, note was taken of the temperature at which annealing first occurred, and measurement of the other crystals of that material was restricted to lower temperatures.

Once the lifetime had been determined for a sample as a function of reciprocal temperature, the data were plotted on semilog paper, and a

smoothed curve was drawn through the data points. Each set of points $(\frac{10^3}{T}, \tau_m)$, where τ_m is the measured lifetime, was identified by a code number affixed after the sample number, indicating the total number of irradiations that had been made on the sample. Thus, E5-0 indicates a pre-irradiation measurement, and E5-2 indicates the second post-irradiation measurement.

By assuming that Eq. (2) holds for any number of sets of recombination centers provided the concentrations of all are small enough, the radiation induced lifetime was obtained from the lifetimes measured before and after irradiation. Equation (2) can be specialized to

$$\tau_m^{-1} = \tau_b^{-1} + \tau_s^{-1} + \sum_{j=1}^{m} \tau_{\gamma j}^{-1} = \tau_0^{-1} + \sum_{j=1}^{m} \tau_{\gamma j}^{-1} \tag{5}$$

where τ_b is the pre-irradiation bulk lifetime, τ_s the effective surface lifetime, $\tau_{\gamma j}$ the lifetime which would be measured in an infinite sample due to defects induced during the jth irradiation, and τ_0 the pre-irradiation lifetime. Thus the radiation induced lifetime due to the first two irradiations in sample E5 is given by $\tau_\gamma(2,0) = (\tau_{\gamma 1}^{-1} + \tau_{\gamma 2}^{-1})^{-1} = (\tau_2^{-1} - \tau_0^{-1})^{-1}$. Each set of points $(10^3/T, \tau_\gamma(m,n))$ was defined as a data set, and is identified by the sample code followed by the two irradiation numbers m and n, so that in the above example the data set designation is E5-2-0. The values of τ_m and τ_n used to calculate $\tau_\gamma(m,n)$ were obtained from the smoothed curves of τ_m and τ_n at evenly spaced values of $10^3/T$.

The error in the radiation induced lifetime due to the assumption inherent in Eq. (5) that the surface lifetime in independent of the other lifetimes was estimated to be less than 3%, on the basis of the

study of Blakemore and Nomura.[34] This error arises because the lifetime

was measured in the interval from one to four half-decay times of the

photoconductivity, and the effective surface lifetime increases as the

higher order surface decay modes die out. This measurement period for

the later irradiation measurements thus occurred during the period when

the higher order modes were more important than in the pre-irradiation or

lower dose measurements. However, for the high dose measurements, the

surface lifetime was much greater than the radiation induced lifetime,

and hence had less effect upon it. Also helping to reduce the magnitude

of the error was the fact that for the higher dose measurements, in most

cases the lifetime did not vary over more than an order of magnitude in

the temperature range investigated, so that the error in the lifetime

did not change much, and had the effect of a slightly different dose.

A. Analysis of Lifetime-Temperature Data

The changes in the lifetime due to radiation induced defects

were analyzed on an IBM 7094 computer for those cases where measurements

could be made over a temperature range large enough to allow meaningful

interpretation of computer fits to the S-R theory.

The computer program can be described as a "lesser squares

fitting program," in that it adjusts the parameters A_j of the lifetime

formula supplied to it, so that the quantity

$$\chi^2 = \sum_{j=1}^{N} \left(\frac{\tau_j - \tau_{\gamma j}}{W_j} \right)^2 \tag{6}$$

is constantly reduced. In the above expression the sum runs over the N

data points $(10^3/T_j, \tau_{\gamma j})$, W_j is the estimated probable error or the jth

value of $\dot{\tau}_{\gamma j}$, and τ is the lifetime calculated for the temperature of

$10^3/T_j$. The W_j were arbitrarily chosen to be equal to $\tau_{\gamma j}/20$, since the

error in the lifetime measurement is a percentage error. It was also

possible to weigh a given temperature region by increasing the density

of data points in that region, so that that region contributed more to

χ^2 than the other region(s). With the weights as chosen, χ^2 should be

equal to the number of points less the number of parameters if the random

error is 5%.

The vast majority of data were taken at temperatures for which

the approximation $n_o + p_o = n_o(p_o) = N_d'(N_a') = N_d - N_a(N_a - N_d)$ for

n-type (p-type) material was valid to better than 1%. Under these condi-

tions the SR formulae become

$$\tau = \tau_{po}[1 + n_1/N_d' + \tau_{no}p_1/(\tau_{po}N_d')] \qquad (7)$$

for n-type, and

$$\tau = \tau_{no}[1 + p_1/N_a' + \tau_{po}n_1/(\tau_{no}N_a')] \qquad (8)$$

for p-type material.

Unless the defect level is within 0.1 eV of midgap, the ratio $\tau_{no}p_1/(\tau_{po}n_1)$

will be much different from one, and it will either dominate or be domi-

nated by n_1/N_d'. When both terms are important, the energy level obtained

from supposing only one to be important will be closer to midgap than the

correct value obtained from including both terms, since n_1 varies as

$\exp[(E_r - E_c)/kT]$ and p_1 as $\exp[(E_v - E_r)/kT]$. The "extra" term will thus have an activation energy greater than half the gap width, and will cause the lifetime to increase at higher temperatures at a rate greater than if only one term were significant. The net result of this additional increase of lifetime at high temperature is to increase the slope of the lifetime-reciprocal temperature curve, and hence place the apparent level position closer to midgap. Thus, only for energy levels indicated to be within 0.1 eV of midgap need all three terms be considered. For shallower levels, if the level is in the upper half of the gap in n-type material, the lifetime will be given by

$$\tau = \tau_{po}(1 + n_1/N_d') \qquad (9)$$

while if it is the lower half of the gap in the same material, it will be given by

$$\tau = \tau_{po}[1 + (\tau_{no}p_1)/(\tau_{po}N_d')] \; . \qquad (10)$$

Results for p-type material can be obtained by interchanging the n's and p's and substituting N_a' for N_d'.

The simplest approximation to Eqs. (9) and (10) is given by

$$\tau = A_1[1 + \theta^{-1.5} \exp(A_2 - 11.6 \times A_3 \times \theta)] \qquad (11)$$

where A_1 is τ_{po}, θ is $10^3/T$, and A_3 is the energy separation of the recombination level from the nearest band edge in electron volts, with the

factor 11.6 arising from the conversion from eV to $^{\circ}$K. This fit was designated PFZ-1 since it appeared to adequately describe the lifetime behavior in high resisitivity p-type float-zoned silicon.

If the level is nearer the conduction band, A_2 will be given by

$$A_2 = \ln[\omega N_c \theta^{1.5}/N_d'] - \beta' \tag{12a}$$

with $N_c\theta^{1.5} = 1.73 \times 10^{20}\ ^{\circ}\text{K}^{-1.5}\text{cm}^{-3}$. If the level lies closer to the valence band, A_2 will be given by

$$A_2 = \ln[(\tau_{no}N_v\theta^{1.5})/(\omega N_d'\tau_{po})] - \beta \ . \tag{12b}$$

The factors β and β' in the above equations arise from the assumption that the position of the recombination level varies linearly with temperature in a manner given by $E_r = E_{ro} + \beta kT$, With E_{ro} the extrapolated energy level position at zero degrees Kelvin, and k Boltzmann's constant. The above equation for E_r measures energies from the top of the valence band, and so when measuring energies from the conduction band edge, the temperature dependence of the energy gap, $\beta_c k$, must be taken into account by means of the relation $\beta' = \beta - \beta_c = \beta + 2.8$, using a value of -2.4×10^{-4} eV/$^{\circ}$K for $\beta_c k$.[35] This conversion must be used for calculating the lifetime for cases when all three terms in Eqs. (7) or (8) are required.

In those cases in which all three of the parameters A_1, A_2, and A_3 are obtainable for a particular level, it is sometimes necessary to use other information to determine which band edge the level is nearest, since it is possible to imagine values of various parameters in Eqs. (12a) and (12b) which would result in the same value for A_2. Previous

determinations of values of the parameters β, β', ω and the ratio τ_{no}/τ_{po}

for defect levels makes it possible to decide under what conditions the

energy level must lie in the opposite half of the gap from the Fermi level.

If β' varies linearly with the separation of the energy level

position from the conduction band edge, as should be the case for a

substitutional impurity, β' would range from zero for a level near the

band edge to 1.4 for a level at midgap. However, Hall effect measure-

ments on the A center indicate that $\omega e^{\beta'}$ is about $\frac{1}{4}$,[1,15] and since spin

resonance measurements indicate $\omega = \frac{1}{2}$ for this defect,[12] $\beta' = -0.7$

instead of the value of 0.5 which results from the linear model above,

a discrepancy of about 1.2. Taking this discrepancy as a maximum, if

A_2 differs from $\ln(N_c\theta^{-1.5}/N_d')$ by more than $3E_{ro} \pm 0.7 \pm 1.2$, with the

uncertainty in ω giving rise to the ± 0.7 and the rest of the quantity

giving the uncertainty in β', the energy level must lie in the opposite

half of the gap from the Fermi level. It is also possible for the level

to be in the opposite half of the gap even if A_2 lies within the above

range, due to the presence of the additional quantity $\ln[N_v\tau_{no}/(N_c\tau_{po})]$

which has the range -0.9 ± 3. The use of the value of ± 3 for the $\ln \tau_{po}/\tau_{no}$

is based on previous lifetime measurements which report values ranging

from $+2.25$ to -3.14 for various defects.[16,17] If ω and/or β' are known

from Hall effect and spin resonance measurements, the resultant reduc-

tion in the range of possible values of $e^{\beta'}$ will permit a more definite

level position assignment. Similar considerations hold for levels in the

lower half of the gap.

In several experiments it has been determined that the quanti-

ties τ_{po} and/or τ_{no} are not constant. Bemski[36] reported temperature

dependence of T^n, with n = 1/2, 2, and 7/2, for several of the levels

of gold in silicon, and by investigating the injection level depen-

dence of the silicon A-center, Galkin et al[16] concluded that the

electron capture cross-section was strongly temperature dependent

above 250°K. A replot of these data suggests that a reasonably good

fit can be obtained with $\tau_{no} = \tau_{noo} T^{-1/2}(1+\exp(11.5-3.40)$. Baicker's[17]

injection level curves also indicate a temperature dependence for

$\tau_{no} + \tau_{po}$. In view of these findings, a fit allowing for such a

temperature dependence was used when it was suspected that τ_{no} and/or

τ_{po} were temperature dependent. Such fits were designated PP-1 and

PFZ-2.

In the n-type float-zoned samples it is evident that either

2 separate levels or a multivalent level controls the lifetime. The

data sets for this type of material were fit by

$$\tau = PQ/(P+Q) \tag{13}$$

where P and Q are PFZ-1 fits. If both levels are closest to the same

band, the A_2 of P and A_2 of Q are related. Since it was not possible

to measure the lifetime at temperatures low enough that the approxi-

mation

$$\tau \sim \tau_{po} \frac{N_c}{N_d} e^{\frac{-(E_c - E_r)}{kT}} \tag{14}$$

was not adequate for the shallower level, it was not necessary to

take explicit account of the differences (if any) in the degeneracies

of the two levels. Fits NFZ-1, NFZ-2, and NFZ-3 are bilevel fits of

this type.

In the p-type pulled samples it became evident that two levels were active in the recombination process, and fits NFZ-1 and PP-1 were used on these data sets. Fit PP-2 is also of the same form as Eq. (13) with P a PFZ-1 fit and Q a PP-1 fit.

For the high resistivity samples at high temperature, the approximation $n_o(p_o) = |N_d - N_a|$ in n-type (p-type) material is no longer valid. Fit NI-1 was programmed to account for this.

Table 3 lists the various fits used in the analysis of the data, along with their formulae.

B. Annealing

Although some lifetime samples were inadvertently annealed in situ during lifetime measurements, most of the post-anneal lifetime versus $10^3/T$ data were taken after the samples had been annealed by placing them in an aluminum capsule sealed by a teflon O-ring and submerging it in a controlled temperature (± 0.5 ^{o}C) diffusion pump oil bath. For anneals at temperatures above the melting point of the In electrodes the samples were tightly wrapped in Al foil to keep the In in place before being placed in the capsule. Due to the low temperature of the anneals, and the extremely low diffusion constant of In in Si, it was assumed that no In diffused into the Si. At the end of the annealing time the capsule was removed from the bath and opened and the sample dropped into a Freon 11 bath. The same technique was used in performing the isochronal anneals.

C. Hall Effect

Hall measurements were made on bridge-shaped samples cut ultrasonically from wafers approximately 1 mm thick. Electroless Ni contacts were used. Hall voltages were measured at 7 koe from low temperature up to the maximum temperature of measurement ($370^{o}K$ to $400^{o}K$), with initial and final readings taken at $297^{o}K$ to determine any evidence of annealing during the measurement.

The irradiations on the Hall samples were performed at the Oak Ridge National Laboratory.

IV. RESULTS

A. N-Type Float Zoned Silicon

1. Post-irradiation results

On the basis of combined evidence from lifetime and Hall effect measurements, defects introduced by Co^{60} irradiation into n-type FZ silicon have energy levels at approximately $E_c-0.17$ eV and $E_c-0.42$ eV, with the possibility existing that additional levels at about $E_v+0.4$ eV were also created. The lifetime-reciprocal temperature data sets were analyzed by computer on the assumption that only two levels, one near a band edge and one near midgap, were effective in the recombination process. Representative data sets are shown in Figs. 1 and 2, and the formulae used to obtain the calculated curves, along with the parameter values, are listed in Table 4. Not all the computer results are listed, since for some data sets several different

formulae were used to fit the data, but there was no significant difference in the results. This is seen by comparing the results of using a PFZ-1 and NFZ-2 fit for the C4-2-0 data set.

Two attempts were made to test the adequacy of the NFZ-1 and NFZ-2 fits. The quantity $\tau_{po} = (\sigma_p N v_p)^{-1}$ was assumed constant in the above fits, implying a hole capture cross section temperature variation of $T^{-1/2}$, since v_p is proportional to $T^{1/2}$. The NFZ-3 fit which assumes σ_p constant was compiled and used on the data set L5-2-0. This data set, and also the B3-2-0 data set, were also used to test the appropriateness of the more complicated two level life-time formula of Wertheim,[28] which he showed should be used unless the recombination center concentrations are sufficiently small. In both cases the NFZ-1 and NFZ-2 fits were judged to be superior or equivalent to the more complicated formulae, and thus adequate for describing the data.

As is evident from the figures, the shallow level does not have a great effect upon the lifetime in the temperature range investigated, and therefore the parameters calculated for it are much more uncertain than for the deeper level. Since the lifetime could not be measured at temperatures low enough that it approached a constant minimum value, the parameter A_2 in the NFZ-2 and NFZ-3 fits was determined by the deeper level. In the NFZ-1 fits the value of A_2 for the shallow level appeared to be determined essentially by the original estimate required by the computer program. It was therefore impossible to determine from lifetime measurements alone which band edge the recombination level was nearest. The lifetime was not measured

for $10^3/T$ greater than 4.5 because of the effects of trapping at low temperatures. Strong trapping strictly invalidates Eq. (2), and it is thus impossible to correct for trapping unless the trap position and concentration are known. Since these quantities were not known, the lifetime was not measured when trapping was manifestly important. Naturally it is impossible to determine at what point trapping begins to significantly affect the lifetime, and hence at high $10^3/T$ trapping may have caused it to increase above the value predicted by the simple SR theory. This would cause the shallow level position to appear to lie closer to the band edge than it would in the absence of trapping. The estimated error in the shallow level position is about 0.05 eV.

All the parameters for the deep level could be determined from the lifetime measurements, with an accuracy roughly proportional to the resistivity of the material. Assuming the level to be nearer the conduction band, its position, on the basis of all runs on all samples, is at $E_c - 0.42\pm0.03$ eV. The difference between A_2 for the deep level and $\ln [N_c \theta^{-1.5}/N_d{}']$, theoretically equal to $\beta' + \ln \omega$, ranged from -0.76 to 3.41 (Table 4). Since this level is suspected of being the E center, $\ln \omega$ is 0.7, and most of the values of $A_2 - \ln [N_c \theta^{-1.5}/N_d{}']$ fall within the predicted range of 1.9 ± 1.3, so that the level position is not restricted to being in the lower half of the gap.

The divacancy has been reported to have energy levels near this position, and it was deemed appropriate to determine the effect of the multi-leveled divacancy upon the lifetime. Eqs. (3) and (4)

were therefore used to calculate the lifetime due to divacancies, and since the various capture cross-sections are not known, the following values were used: level 1 at E_v + 0.25 eV, $\omega = 2$, $\tau_{po} = 20$, $\tau_{no} = 1$; level 2 at E_v + 0.45 eV, $\omega = 1/2$, $\tau_{no} = 20$, $\tau_{po} = 1/2$; level 3 at E_c - 0.4 eV, $\omega = 2$, $\tau_{po} = 1/2$, $\tau_{no} = 20$. The level positions were those given by Watkins and Corbett; the values of ω were deduced from their model, and the values of τ_{no} and τ_{po} from the charge states of their model. The results of this calculation, with N_d, appropriate for 200 ohm-cm n-type material, were analyzed with the PFZ-1 program to indicate a level at about the same position with a slightly lower value of ω (1.5). At least for the above model, the lower level of the divacancy does not contribute much to the recombination process.

The parameters for the deep level can equally well be inter- preted as belonging to a monovalent level at E_v + 0.42 eV which has a larger hole than electron capture cross section (indicative of a defect with neutral and negative, or negative and doubly negative charge states). A more probable possibility, on the basis of evidence presented below, is that recombination occurs through two or more deep levels, whose net recombination rate appears to be that of the levels proposed above. A difference in introduction rates between the two levels, due to variations of impurities and dislocations in and between boules, would then explain the large variation seen in the parameter A_2 for the deep level.

The lifetime energy level positions appeared to be deeper in the gap for succeeding irradiations, most particularly in the case

of the shallow level, where the energy level appeared to be about

0.1 eV from the band edge in all but the L3 data set after the first

irradiation. This shift of energy levels to larger separations indi-

cates that best results are obtained when the pre- and post-irradiation

lifetimes differ greatly, and when the post irradiation lifetime is

dominated by radiation induced defects. Anomalous results, compared

to other materials of the same impurity group, were often obtained on

samples having a very low pre-irradiation lifetime, such as the B, P,

and R samples.

Hall effect measurements on material from boule B indicated

that an exposure dose of 3.1×10^7 r introduced $4 \times 10^{13} cm^{-3}$ deep

levels and 3.8×10^{13} shallow levels. The energy level positions

determined from the Hall measurements were deeper in the gap by

about 0.03 eV than the lifetime levels, but the shallow level was

about 0.03 eV shallower than reported by Sonder and Templeton.[2] The

acceptor levels created in the two Hall samples from the C boule

appeared to be 0.01 to 0.02 eV deeper than in the B material, and in

good agreement with the Sonder and Templeton findings. The average

introduction rates for levels in the C samples, defined by $\langle dN/d\phi \rangle =$

N/ϕ, were $7.7 \times 10^5 cm^{-3} r^{-1}$ for the shallow level in the C-A sample

(exposure dose 1.1×10^7R), and $4.7 \times 10^5 cm^{-3} r^{-1}$ and $4.1 \times 10^5 cm^{-3} r^{-1}$

for the deep level(s) in the C-A and C-B (exposure dose 3.1×10^7r)

samples, respectively. Since these measurements, as well as those

reported by Sonder and Templeton, and Saito, Hirata, and Horiuchi,[4]

were performed on materials of resistivity such that complete ioni-

zation from the deep level could be observed only at temperatures for

which annealing of the defects occurred, it is not possible to state

that divacancies or other deep defects, were not also created in

addition to E centers. Very high resistivity material ($\rho \geq 2000$

ohm cm) would be required for such a study.

Using the above introduction rates for the deep levels,

and assuming that recombination occurs mainly through the E center,

the E center hole cross-section was calculated using the lifetime-

flux products ($\tau_{po}\phi$) for this level. The hole thermal velocity at

250°K, 1.5×10^7 cm/sec, in conjunction with the definition of τ_{po} and

the above-mentioned quantities $\langle \tau_{po}\phi \rangle$ and $\langle dN/\phi \rangle$ enables one to calcu-

late

$$\sigma_p = (N \tau_{po} V_p)^{-1} = [(N/\phi)(\tau_{po}\phi) V_p]^{-1} .$$

The resulting hole capture cross-section is 2.5×10^{-14} cm^2 and

5.2×10^{-14} cm^2 for the B and C materials, respectively.

2. Post anneal results

The annealing of the deep levels at low (100°C) temperatures

is seen in Fig. 2, which shows the function f versus the annealing

temperature for n-FZ samples, where f is given by

$$f = (\tau_A^{-1} - \tau_o^{-1})(\tau_m^{-1} - \tau_o^{-1})^{-1}, \tag{15}$$

with τ_A the post anneal lifetime, τ_o the pre-irradiation lifetime,

and τ_m the post-irradiation lifetime, all measured at room tempera-

ture. If only one type of defect is present, and if it anneals without

creating any other recombination centers, then f can be shown to be the fraction of recombination centers not annealed.

The observed behavior of f for the samples B2, L5, and C3 can qualitatively be described as due at least two types of defects: those which account for the major part of the radiation induced lifetime and which anneal by $200^{o}C$, and another type which anneals at a higher temperature. The differences in the high temperature annealing are suggestive of several defects annealing in this range rather than just one, and the lesser differences in the low temperature annealing might also indicate several levels, but more probably are due to differences in dislocation content or similar factors which could affect the annealing.

Figure 3 shows the lifetime $-10^3/T$ data sets for sample B3 and C4 after the indicated anneals. Due to the scattered nature of the B3 data sets, no attempt was made to fit curves to them. The C4-4A2-0 data set, according to Eq. (2), gives information on all defects present after the anneal, including the un-annealed radiation induced defects and those created from the constituents of the annealed defects and other impurities in the crystal. Computer calculations performed to obtain the curve indicate, 1) most deep levels anneal at a low temperature, but a small fraction, apparently slightly deep in the gap than the others, are more stable, 2) annealing either "shifts" the shallow level position form 0.17 eV to 0.22 eV from a band edge, or creats defects with the latter energy separation, and 3) the lifetime-flux product of the remaining deep levels based on the assumption that all the less stable defects and none of the more stable defects

have annealed, is about 120 sec-r, compared to the 2 or 3 sec-r for the less stable defects. Evidence for this assumption comes from the small (13%) change seen between the first (13 hr at 145°C) and second (20 min at 250°C) anneal treatments.

B. Phosphorus Doped Crucible Grown Silicon

    1. Post irradiation results

An examination of the data sets (Fig. 4) of the irradiation induced lifetime in the n-type pulled materials suggests that the behavior of these materials is the same as that of the n-type FZ samples, except that trapping affects the lifetime in all cases for temperatures below 300°K.

The energy separation values obtained from the slopes of the lines through the H2 data sets (Fig. 4a) are somewhat low compared to that expected for recombination due to A centers alone (0.24 eV at $10^3/T = 2.9$), but if recombination through the deeper levels seen in the higher resistivity materials (I, T) is also assumed to take place in this material, then the net lifetime calculated for this material fits the data set H1-1-0 very well. The shallow level position at zero temperature E_c- 0.175 eV) and degeneracy ratio-temperature dependence product $\omega e^{\beta'}$ ($e^{-1.4}$) used were those of Sonder and Templeton,[1] for the deep level, parameters close to those determined above for the deep level in sample C4 were used ($E_r = E_c$- 0.42 eV, $\omega e^{\beta'} = e^{0.78}$). τ_{po} for the shallow level was estimated from the A center introduction rate found in the B Hall sample, in accordance with the findings of

Sonder and Templeton[2] that the A center introduction rate is not strongly dependent upon the oxygen concentration, and from the hole capture cross section found by Galkin et al.[16] τ_{po} for the deep level was estimated from the lifetime results on the I and T7 crystals. The τ_{po}'s (48 and 0.29 μsec for the deep and shallow levels, respectively) were than adjusted slightly to give the fit shown. A computer fit was not used in this case.

Trapping appeared to affect the radiation induced lifetime in the H2 sample more than in the H1 sample, as is evidenced by the decrease in slope of the lifetime with decreasing temperature for the H2 data sets. The near-constancy of the lifetime at $10^3/T = 3.3$ in the H1 data set is attributed to the temporary pinning of the Fermi level at $E_c - 0.32$ eV due to the ionization of electrons from deep donor levels, whose concentration was found to be about $8 \times 10^{13} cm^{-3}$ by Hall measurements on a sample of unirradiated H material. Photoconductivity measurements at room temperature have shown that the donors are characterized by very low electron and high hole capture cross-sections, where the hole capture time was too short to measure while the electron capture time was of the order of seconds. The electron capture time increased with decreasing temperature, and at nitrogen temperature was greater than tens of minutes.

A resistivity variation across the diameter of the T boule (80 ohm-cm at the center, 8000 ohm-cm at the periphery) was discovered, and the lifetime samples used were therefore cut with their long dimensions along the boule axis rather than a boule diameter. Sample

T4, cut from the center of the boule, had a resistivity of sample T7,

cut from a region farther from the center, varied by a factor of two

along its smallest dimension, which was a boule diameter, and less

than 5% in the other dimensions.

Hall effect measurements on a similarly cut sample of 195

ohm-cm material from boule T revealed that the Hall mobility of

electrons was very low (1100 cm^2/volt-sec at $300^\circ K$ compared to 1500

to 1600 cm^2/volt-sec in the other n-type materials), and that two

groups of deep levels existed in this material prior to irradiation.

Shallow donors, at E_c- 0.15 eV, were present in a concentration of

$10^{13} cm^{-3}$, but since the pre-irradiation lifetime was controlled by

surface recombination, it is evident that these levels are not A

centers. Deeper donors, with energy levels apparently ranging from

E_c- 0.37 eV to E_c- 0.47 eV, with a total concentration of slightly

more than $10^{13} cm^{-3}$ were also seen. Comparison of the Hall effect

measurements before and after exposure of the sample to a dose of

10^8 R indicated that approximately 4.5 $\times$ $10^{12} cm^{-3}$ deep acceptors,

located at least 0.45 eV from the conduction band edge, were created,

as well as more A centers than donors.

The radiation induced lifetime behavior of sample T4

(Fig. 4a) can be fairly well described by recombination through two

levels, one due to the A center, with the parameters as given for the

H1-1-0 data set, and a deeper level, 0.45 $\pm$ 0.04 eV from a band edge.

τ_{po} for the deep level was found to be 38 μsec, and $\omega e^{\beta'}$ to be

4.5 $(e^{1.5})$, which can be interpreted as a conduction band level with

$\omega = 2$ and $\beta' = 0.8$, or a valence band level with $\sigma_p \gg \sigma_n$. A constant electron concentration was assumed in the above calculation, which was done with the NFZ-2 program in the region where trapping did not affect the lifetime when the non-additivity of radiation induced lifetimes was observed.

The lifetime results on the T7 crystal were in rough agreement with the T4 results, but were not computer analyzed because the large resistivity variation across the sample would case doubt on the validity of the parameters obtained.

The hole capture cross section for the deep level seen in this material was calculated from the lifetime-flux produce of the T4-2-0 data set and the Hall introduction rate for deep levels to be about $8 \times 10^{-15} cm^2$.

Figure 4b shows the temperature behavior of the radiation induced lifetime for data sets I4-1-0 and I4-2-0 as well as data sets taken on crystal I1. Although there is little scatter in the data, trapping affects the lifetime for $10^3/T$ greater than 3.4, and there is considerable difference between the data sets I4-1-0 and I4-2-0 for all $10^3/T$, indicating that Eq. 2 does not apply to the lifetime due to defects introduced by the second irradiation, and hence not for the first irradiation either. The parameters for the curves fit to the data sets are thus not useful for precise interpretation. The PFZ-1 parameters for the curve through the data set I4-1-0 are $A_1 = 19.37$, $A_2 = 14.06$, and $A_3 = 0.358$. The NI-1 parameters for the curve fit to the I4-2-0 data set can be converted to PFZ-1 parameters for $10^3/T = 2.65$ and are $A_1 = 12.68$, $A_2 = 17.75$, and $A_3 = 0.483$.

Neither fit took into account the effect of A centers upon the life-
time, which was not negligible, since the A center lifetime, calcu-
lated from the T4 and H1 parameters, was less than six times the
measured lifetime over the range of measurement.

2. Post anneal results

The results of the 10 minute isochronal anneals, shown in
Fig. 5, indicate that the behavior is determined by unmonitored fac
factors, such as concentrations of impurities other than phosphorus
or oxygen, or dislocation content. The behavior of crystal I4 below
220°C is quite similar to that of the float zoned samples, particu-
larly L5, but at higher temperatures defects appear to be created.
Sample I1 was heat treated at 400°C and a decrease of resistivity was
found, probably the oxygen related donors reported previously, con-
firming the formation of defects at high temperatures. The removal
of A centers during a 6 hour anneal at 250°C was indicated by measure-
ments on sample I1 after a total dose of 2×10^{7} r (data set I1-3A1-
3A2, Fig. 4b). Qualitative features from other runs indicated that
annealing of the deeper levels occurred during measurements at tem-
peratures below 160°C.

The behavior of the annealing of the lifetime in sample T7
appears to be due to the annealing of the deeper levels, which do not
anneal at temperatures below the temperatures at which annealing of
the A center is seen in sample I1 and in other studies. The A center
has only a small effect upon the lifetime in this material due to

The high resistivity, and its anneal is therefore not expected to be seen. The anneal appears to be complete in this sample at about the same temperature as in sample B2.

The behavior of the annealing in the H2 sample is due to poisoning from the nickel electrodes, which were left on during the 120 and 140°C anneals only.

C. P-Type Float Zoned Silicon

1. Post irradiation results[37]

The variation of radiation induced lifetime with reciprocal temperature in this class of material indicates that recombination is either due to a multivalent defect, such as the divacancy, or two monovalent defects. The first possibility will be seen to be untenable when this type of material is compared to p-type pulled material, and so the results were analyzed on the basis of two monovalent defects.

The data sets for the higher resistivity materials indicate that one of the recombination levels is in the upper half of the gap, with a larger hole than electron capture cross section. Figure 6a shows representative data sets for the F and U samples, and the parameters for the curves are given in Table 5. In F data sets were fit best with τ_{no} and τ_{po} constant. In the U, and M data sets shown in Fig. 6b, τ_{no} appeared to have a temperature dependence of T^n, with

n between 0 and 1. In all cases the level appeared to be about 0.33 eV from the conduction band edge. Since annealing of the defects prevented measurement of the lifetime at temperatures high enough that the lifetime increased exponentially, the exact level position is uncertain by as much as 0.1 eV.

A second level can be seen to be effective in the E material. The results from the higher resistivity materials were used to determine the parameters for the deep level, which were held fixed in the calculations determining the shallow level parameters. These results, on the data set E5-2-0 and the combined data sets E4-2-0 and E3-1-0, indicate that the shallow level is 0.17 eV from a band edge, with $A_2 \approx 10$. The latter parameter can be interpreted either due to a level near the valence band edge with $\omega \, e^{\beta} = 1.4$, according to Eq. (9), or due to a level the same distance from the conduction band edge with $\omega \, e^{\beta'} \sigma_n / \sigma_p = 0.1$, according to Eq. (10). If $\omega \, e^{\beta'}$ is assumed to be 4, then σ_p / σ_n is approximately 40, while if it is 1/4, σ_p / σ_n will be about 2.5.

If the introduction rate observed in the E samples for the 0.17 eV level is assumed to hold for the other materials, Eq. (2) predicts that this level will be unobservable in all but the M samples because of their higher resistivities. In the M samples, the 0.3 eV level is expected to control the lifetime except at very low temperatures, where trapping affects the measurements.

In calculating the lifetime-flux products $\tau_{no} \phi$ for these materials, it is necessary to specify temperature on account of the

temperature variation of τ_{no}. A slight correlation between the life-time-flux products for the 0.3 eV level and the 9 micron (oxygen) absorption band indicated that the rate formation of these defects was greatest in the most oxygen free samples. The lifetime flux products for the deep level, at $10^3/T = 3.4$, were 700 sec-r., 70 sec-r., 109 sec-r for the E, M, and F samples respectively, and 47 sec-r for doses less than 10^7 R, and 66 sec-r for a total dose of 10^7 sec-r in the U samples. The lifetime-flux product of the 0.17 eV level in the E samples was about 40 sec-r.

2. Post-anneal results

The annealing behavior of the samples is seen in Fig. 7, where the plot of f, the fraction of the radiation induced recombination rate not annealed, against temperature indicates that in the M and U samples the defects do not anneal out below 340°C, and in the M sample, the heat treatment has created recombination centers. Negative anneal in the E sample is evident, and is probably connected with the low temperature anneal in the U and F materials, i.e., constituents of the defect breaking up at about 120°C form recombination centers with other defects in the crystals.

The variation of lifetime in the E, M, and F samples with temperature after various annealing treatments is shown in Fig. 8.

The E4-2A data set was taken nine months after the E4-2 data set, after a twenty minute, 200°C anneal. The lifetime was measured at room temperature before the anneal, and it was seen that negative anneal had occurred at room temperature, since the lifetime had

decreased from 32 to 18 microseconds during the nine month period. The subtracted data sets E4-2A-0 and E4-2A-2 were calculated, and were analyzed by computer. The data set E4-2A-0, which should be related to all defects present at the end of the anneal treatment, was fit by NFZ-1, but the fit was poor and did not give results consistent with the preanneal results. The data set E4-2A-2, which reflects the changes in the lifetime due to the anneal, were fit well with the PFZ-1 fit to give a level about 0.3 eV from a band edge. A very high temperature dependence of -1.7 eV/^{o}K (compared to -1 eV/^{o}K expected on the basis of uniform level shift with contraction of the bandwidth), with $\omega = 1/2$ is required for a valence band fit, while for a conduction band fit it appears that the electron capture cross section is much larger than the hole capture cross section, exactly opposite to the findings for the radiation induced level seen at this position.

The negative anneal seen in the M4 sample indicates a level about 0.16 eV from a band edge. Due to trapping it was not possible to determine tha parameter A_2 and hence obtain information as to which band edge the level was nearest.

The F4 data sets indicate that in this material the defects may anneal without creating any new defects, since the various data sets resemble each other strongly.

D. P-Type Pulled Silicon

1. Post-irradiation results

The p-type pulled results curves shown in Fig. 9, with parameters listed in Table 6, indicate that the same levels seen in p-type FZ material after irradiation control the lifetime in this material also. The difference in introduction rates between the two materials for the deep level indicates that two monovalent defects and not a multivalent defect such as the divacancy control recombination. The much higher $\tau_{no}\phi$ products for the deep level (of the order of 1000 sec-r.) in this material are in agreement with the conclusion that the presence of oxygen retards the formation of these defects.

The shallow level parameters are best determined by the calculations on sample S2, where the lifetime could be measured nearly to the low temperature limit τ_{no}. The results of the computer calculation can be interpreted as due to a level 0.18 eV from either band. For a valence band level, $\omega e^{\beta} = 2.2$, and if the temperature dependence closest to that predicted by the uniformly shrinking gap model is assumed to be more likely correct, it appears that $\omega = 2$. For a conduction band level, the electron capture cross-section must be much greater than the hole capture cross section, if reasonable temperature coefficient values are to be obtained.

The data sets taken on sample 01 indicated that the shallow level in this material was the same as in sample S2. Trapping at low temperature, and annealing at high temperature made the data, and hence the analysis more uncertain than for S2. The annealing was of the

deeper level, which was indicated by a decrease in the slope of the lifetime at high temperatures. Both the S2 and O1 data sets were fit by the PP and PFZ-1 programs. The PP-1 and PP-2 programs were written to use the temperature dependence of the electron capture cross section found by Galkin, et al.[2] for the A-center, since it appeared that this level might be due to the A-center. For the S2 data sets no difference could be seen between the two fits, as the term did not contribute much to the lifetime. However, in the O1 data sets, the τ_{no} term was appreciable, and the difference between the two fits can be detected in Fig. 9a. The parameters for the PP fits were those determined in the S2 PP fits, and should be applicable for all p-type material. These parameters were essentially those giving the capture cross-section dependence of Galkin.[16]

The P1 and R2 samples showed trapping at low temperature, and annealing at high temperature such that their data sets are best used to qualitatively confirm the conclusions made from the other p-type data sets. The fits to the P1-1-0 and P2-2-0 do not agree with each other, but the P1-2-0 fit agrees well with the other p-type results. The P1-1-0 results are felt to be in error due to using data points at the lower temperatures where trapping affects the lifetime, but most probably because not much change in the lifetime was seen between the P1-1 and P1-0 measurements.

2. Post anneal results

The results of the ten minute isochronal anneals are shown in Fig. 10, and they indicate that the levels in this type of material

anneal much like that in p-type float zoned material. The S2 data
are much like the E3 data, and the O1 data resemble the S2 annealing
data, with a peak of the negative anneal at 200°C. The peak of nega-
tive annealing in sample P1 occurred at 120°C, and a slight negative
anneal at that temperature is also seen in sample O1. No measure-
ments of the lifetime as a function of temperature were made in the
annealed samples, since only one sample of each resistivity of this
material was used, compared to the several samples of each resistivity
of the other types of materials.

V. DISCUSSION

A. N-Type Material

The positions of the levels and the annealing behavior of
the defects studied in this experiment in a large variety of phos-
phorus doped silicon crystals agree well with those previously reported.
The shallow level at $E_c - 0.17$ eV, on the basis of previous Hall,[1,2,5]
spin resonance,[12] and infrared absorption experiments,[38] was considered
to be due to the Si-A center. Of somewhat greater interest were the
deeper levels seen. Substantial difference was seen between pulled
and FZ material in the lifetime results.

In FZ material, after irradiation the apparent lifetime
level position of $E_c - 0.42$ eV was in good agreement with the reported
results of Glaenzer and Wolf,[19] Nakano and Inuishi,[13] and Hirata et al.[21]
While the anneal of the lifetime seen in this experiment was very

similar to that reported by Nakano and Inuishi the slope of the life-time-reciprocal temperature curves shown in their paper indicates a much shallower level than $E_c - 0.4$ eV. Although Nakano and Inuishi attributed this to the effects of trapping, it is more probably the result of ending measurements at a high temperature of 300°K, as can be seen by comparing their lifetime curves to those for sample L of this experiment, or the 77 ohm cm sample of Glaenzer and Wolf, all of which have roughly the same resistivity. L5 and Glaenzer and Wolf curves show that for $10^3/T = 3.0$ the average slope of the lifetime is very small. Glaenzer and Wolf also reported on a 32 ohm cm sample, and in both samples found it possible to measure to 135°C with no evidence of anneal. This is in agreement with the results of annealing on sample L5, but not with those for B2, C3, or the samples of Nakano and Inuishi, and hence indicate that the exact annealing temperatures in a given crystal depends on other factors, perhaps dislocation content, as is indicated by Nakano et al for p-type FZ silicon.[20] The data of Glaenzer and Wolf were analyzed by the NFZ-2 program, and the results indicated the level positions to be slightly deeper than reported by them by about 0.02 eV.

When both lifetime and Hall data are available on the same samples, it is easier to ascertain which half of the gap the lifetime levels are in, since if the recombination and Hall acceptors are identical, comparison can be made between their temperature dependences, which depend on the same parameters. Saito and Hirata have obtained data by both methods,[4,20] and if one presumes to compare results for samples of nearly the same resistivities, it becomes apparent that

their lifetime data are controlled by levels in the lower half of the gap. This must be because 1) ionization is not seen in their 46 ohm cm material for $10^3/T \geq 2.6$ (Hall study)$(n_1 \ll n_o)$, 2) the lifetime in one of their 50 ohm cm samples is in its high temperature form at $10^3/T = 4.0$ $(n_1 \gg n_o$ for conduction band level), and 3) ionization is seen in 140 ohm cm material, indicating the Hall level is the upper half of the gap. The level seen by Hirata et al could possibly be the one seen by Curtis[39] in neutron irradiated material. In the present study, the temperature dependences of the lifetime and of the Hall coefficient were seen to be the same in all cases (B, C, and T materials).

The hole capture cross section values reported herein are felt to be superior to those previously reported for several reasons. The value of Glaenzer and Wolf $(9 \times 10^{-14} \text{cm}^2)$ was obtained using the introduction rates of Saito et al,[4] and the value of Nakano and Inuishi $(5 \times 10^{-14} \text{cm}^2)$ were obtained with the use of lifetime data that did not clearly show the value of τ_{po} for the deep level. The value of Hirata et al $(1.1 \times 10^{-13} \text{cm}^2)$ should perhaps be better than the others since it was obtained from Hall and lifetime measurements taken at the same laboratory, and perhaps on the same crystals. However, the unusual temperature behavior of their data makes it unlikely that the capture cross section measured is for the E center. The present values of 2.5 and $5.2 \times 10^{-14} \text{cm}^2$, are therefore felt to be more accurate. Since it appears probable that at least two types of defects with levels at about the same position are involved, the value obtained is thus an average over all of the deep levels. It is

therefore pertinent to note at this point the hole capture cross section value of the deep level in the T material of $8 \times 10^{-15} \text{cm}^2$, which is about 1/3 of the value for FZ material. Using the introduction rate of deep centers in the T sample as characteristic of the second deep level, the corrected value of the hole capture cross section in the comparable FZ material, C, is increased only by about 10%.

The last feature worthy of note in FZ material is the creation of defects with energy levels at $E_c - 0.23$ eV by anneal of the E centers, seen in the data set C4-4A2-0. This has previously been seen in the Hall effect by Sonder and Templeton,[2] but not in lifetime studies.

The pulled n-type results also indicate recombination levels at $E_c - 0.17$ eV and at about $E_c - 0.4$ eV in all samples. The annealing results on samples I4 and T7 indicate that in sample I4, E centers as well as the other center with a deep level were formed. An indication of annealing of the E centers was seen, in contrast to sample T7, where essentially no anneal took place below 300°C. The speculation that the defect in sample T7 was the divacancy is contradicted to some extent by the divacancy anneal data reported by Watkins and Corbett,[14] who found that the divacancy annealed in FZ material at temperatures somewhat (50°C) higher than in pulled material. This is the reverse of the behavior observed in this experiment for the high temperature annealing of the deep level.

The level at E_v + 0.27 eV reported in low resistivity electron-irradiated material reported by Wertheim[15] and by Baicker[17] was not seen, which suggests it is related to some impurity present in their material but not in material used by Glaenzer and Wolf, or in this investigation.

B. P-Type Material

The previously reported lifetime results in p-type material do not correlate well with one another, Hall effect,or photoconductivity results. Wertheim[15] reported a recombination level at E_c - 0.18 eV in 5 ohm cm electron-irradiated material, and a Hall donor level at E_v + 0.27 eV. Re-evaluation of his published lifetime data by the present computer analysis indicates the recombination level was most probably at E_v + 0.25 eV, in fair agreement with his Hall measurements. Baicker[17] reported recombination levels in 1 to 2 ohm cm electron irradiated material to be at E_v + 0.18 eV in both pulled and FZ material. His experimental technique enabled him to study the life-time as a function of injection level, $\delta p/p_o$, where δp is the density of excess carriers. His results indicate that this level is defi-nitely in the lower half of the gap, and not the A-center, as Wertheim had supposed his level at E_c - 0.18 eV to be. The data for Baicker's N341 sample was analyzed by the PFZ-1 program, and it was found that the difference between A_2 and $\ln[N_v(10^3/T)^{-1.5}/N_a']$, which will be $e^{-\beta}/\omega$ for a valence band level, was the same as determined for the sample S2 in this experiment, indicating that the levels seen by

Baicker in low resistivity material are the same as seen in similar material in this study.

Nakano et al[20] reported recombination levels at E_v + 0.21 eV for pulled material, and at E_v + 0.27 eV for FZ material. However, analysis of their published data indicates a level 0.06 eV from a band edge, after a correction is made for the temperature variation of the density of states of the valence band, with the change from low temperature to high temperature behavior occurring at higher temperatures as the total dose increased. Since they used heavy doses, this effect is in accord with the predictions of Wertheim and Sandiford, but even so, the slope of the lifetime at high temperature should give the level position correctly. Disregarding the level positions reported by Nakano et at, their lifetime annealing results are in good agreement with the present results, showing a negative anneal at about 220°C in all pulled samples. In their FZ samples, evidence of partial annealing at low temperatures was also seen. This suggests that the same level was indeed observed in both cases, but that the level positions reported by Nakano et al were probably in error. Of course, the similarity in annealing might be coincidental, with different defects involved in the two studies.

The most recent report on lifetime in p-type material, Hirata et al,[21] professed to see recombination in both pulled and FZ material occurring through A centers. Their level positions were obtained by measuring the slope of lines drawn through the high temperature post-irradiation data. The lifetime results for their FZ crystal show that the pre- and post-irradiation lifetimes converge

at high temperature, and hence a correction must be made for the pre-irradiation lifetime. When this correction is made, a level position about 0.3 eV from a band edge is found for the defect in this material. Analysis of the parameters indicates that it is more likely nearer the valence band, and hence is unlike any levels seen in this experiment. The results of Hirata et al on pulled material, after correction for the pre-irradiation lifetime, indicate a level near the conduction band, but somewhat shallower (E_c - 0.12 eV) than the A center. It thus appears that the A center is not seen in p-type material, but that a level at about E_v + 0.18 eV is often seen.

Since Whan[40] has shown that the A center introduction rate is probably less in p-type than in n-type material and since the τ_{no}/τ_{po} ratio is much larger than one for the A center, it would be expected to be less effective than the recombination levels at E_v + 0.18 eV in controlling the lifetime. Hence the presence of A centers would be masked by the other defects.

Also, if the recombination levels seen in p-type material are related to the boron concentration, then these levels would not be observed in n-type material. By analogy with the models proposed for n-type material, the level at E_v + 0.18 eV would be due to a defect comprised of oxygen, boron, and perhaps interstitials or vacancies, while the level at E_c - 0.3 eV would be due to defects involving boron and interstitials or vacancies.

Comparison of the lifetime results to the Hall effect results on p-type material indicates that the major Hall donor levels at E_v + 0.21 and E_v + 0.28 eV seen by most investigators are not

active in the recombination process, but that the Hall E_v + 0.18 eV level seen after annealing is probably the recombination level seen in pulled and low resistivity FZ material.

VI. SUMMARY

1) The recombination levels in n-type Si appear to be the A center, the E center, and another deep level at about E_c - 0.4 eV. The defect responsible for the latter level could be the divacancy. The introduc rate of the A center and of the defect with level at E_c - 0.4 eV is nearly independent of the material. The E center introduction rate is dependent upon the phosphorus and oxygen concentrations.

2) The capture cross sections of the two deep levels for holes were found to be 8 $\times$ 10^{-15}cm^2 for the suspected divacancy, and between 2.5 and 5 $\times$ 10^{-14}cm^2 for the E center.

3) The recombination centers in p-type material were found to be at E_v + 0.18 eV and E_c - 0.3 eV. No correlations with acceptor concentrations could be made for the shallow level. The introduction rate for the deep level was quite sensitive to the concentration of oxygen.

4) The effect of oxygen in the lifetime p-type gamma irradiated silicon is the same as that seen previously in n-type material. In oxygen containing material the dominant levels induced at room temperature by gamma irradiation are those located close to a band

edge, while in FZ silicon the dominant levels are deeper in the gap.

5) Annealing at $250^{\circ}C$ was found to remove the E centers in n-type material, and to introduce recombination levels at $E_c - 0.23$ eV.

6) Annealing in p-type FZ material was found to remove the $E_c - 0.3$ eV levels, and to introduce other levels. In some material annealing introduced levels at $E_c - 0.3$ eV which had a ratio of capture cross sections opposite to that of the levels annealed out, while in other material levels 0.18 eV from a band edge were introduced, and in still other material, no levels were introduced by the anneal.

VII. ACKNOWLEDGMENTS

REFERENCES

1. E. Sonder and L. C. Templeton, J. Appl. Phys. 31, 1279 (1960).

2. E. Sonder and L. C. Templeton, J. Appl. Phys. 34, 3295 (1963).

3. E. Sonder and L. C. Templeton, J. Appl. Phys. 36, 1811 (1965).

4. H. Saito, M. Hirata, and T. Horiuchi, J. Phys. Soc. Japan 18, Supplement III, 246 (1963).

5. T. Tanaka and Y. Inuishi, J. Phys. Soc. Japan 19, 167 (1964).

6. N. A. Vitoviskii, D. P. Lukirskii, T. V. Mashovets, and V. I. Myakota, Soviet Physics-Solid State 4, 840 (1962).

7. G. K. Wertheim and D. N. E. Buchanan, J. Appl. Phys. 30, 1232 (1959).

8. V. S. Vavilov, G. N. Galkin, V. M. Malovetskaya, and A. F. Plotnikov, Soviet Physics-Solid State 4, 1443 (1963).

9. T. Tanaka and Y. Inuishi, Jap. J. Appl. Phys. 4, 725 (1965).

10. V. M. Malovetskaya, G. N. Galkin, and V. S. Vavilov, Soviet Physics-Solid State 4, 1008 (1962).

11. Y. Inuishi and K. Matsuura, J. Phys. Soc. Japan, 18, Supplement III, 240 (1963).

12. G. D. Watkins and J. W. Corbett, Phys. Rev. 121, 1001 (1961).

13. G. D. Watkins and J. W. Corbett, Phys. Rev. 134, A1359 (1964).

14. G. D. Watkins and J. W. Corbett, Phys. Rev. 138, A543 (1965).

15. G. K. Wertheim, J. Appl. Phys. 30, 1166 (1959).

16. G. N. Galkin, N. S. Rytova, and V. S. Vavilov, Soviet Phys.-Solid State 2, 1819 (1961).

17. J. A. Baicker, Phys. Rev. 129, 1174 (1963).

18. T. Nakano and Y. Inuishi, J. Phys. Soc. Japan 19, 851 (1964).

19. R. H. Glaenzer and C. J. Wolf, J. Appl. Phys. 36, 2197 (1965).

20. T. Nakano, K. Nakasima, and Y. Inuishi, J. Phys. Soc. Japan 20, 2140 (1965).

21. M. Hirata, M. Hirata, and H. Saito, J. Appl. Phys. **37**, 1867 (1966).

22. R. G. Shulman, "Recombination and Trapping," pp. 493-500, in
    Semiconductors, N. B. Hannay, ed., Reinhold Pub. Co. New
    York, 1959, and A. P. Ramsa, H. Jacobs, and F. A. Brand,
    J. Appl. Phys. **30**, 1054 (1959).

23. J. Mandelkorn, L. Schwartz, J. Broder, H. Kautz, and R. Ulman,
    J. Appl. Phys. **35**, 2258 (1964).

24. The earlier designations of Watkins and Corbett are used to
    refer to the defects rather than their more recent scheme,
    which they use to refer to the epr spectra of the defects.
    This is less confusing, particularly when a defect possesses
    more than one epr spectrum.

25. R. N. Hall, Phys. Rev. **83**, 228 (1951).

26. W. Shockley and W. T. Read, Phys. Rev. **87**, 835 (1952).

27. D. Sandiford, Phys. Rev. **105**, 524 (1957).

28. G. K. Wertheim, Phys. Rev. **109**, 1086 (1958).

29. B. G. Streetman, J. Appl. Phys. **37**, 3137 (1966).

30. K. C. Nomura and J. S. Blakemore, Phys. Rev. **112**, 1067 (1958).

31. W. Shockley, Electrons and Holes in Semiconductors, D. Van
    Nostrand Co., Inc., New York, 1950, p. 319.

32. C. -T. Sah and W. Shockley, Phys. Rev. **109**, 1103 (1958).

33. R. K. Swank, Lifetimes of Excited States in Alkali Halide
    Crystals Containing F Centers, thesis, Univ. of Ill., 1962
    (unpublished).

34. J. S. Blakemore and K. C. Nomura, J. Appl. Phys. **31**, 753 (1960).

35. R. A. Smith, Semiconductors, Cambridge University Press,
    Cambridge, Great Britain, p. 350.

36. G. Bemski, Phys. Rev. **111**, 1515 (1958).

37. Some of this material was presented by R. Hewes and W. D. Compton
    at the International Symposium on Lattice Defects in Semi-
    Conductors, Tokyo, 1966.

38. J. W. Corbett, G. D. Watkins, R. M. Chrenko, and R. S. McDonald,
    Phys. Rev. **121**, 1015 (1961).

39. O. L. Curtis, Bull. Am. Phys. Soc. 11, 193 (1966).

40. R. E. Whan, J. Appl. Phys. 37, 3378 (1966).

Table 1

Pre-Irradiation Sample Characteristics[†]

Sample Code	Material Class	Resistivity (ohm-cm)	Pre-Irradiation lifetime (μsec)	Supplier	Notes
B2	nFZ	18	30	D	
B3	"	18	24	D	
L3	"	70	56	M	
L5	"	68	52	M	1,2
C1	"	180	155	D	
C3	"	137	207	D	
C4	"	139	200	D	
C6	"	192	180	D	
H1	nP	25	26	D	3,4
H2	"	26	34	D	3,4
T4	"	79	470	M	2,3
I1	"	220	520	D	3
I4	"	220	87	D	3,5
T7	"	475	290	M	2,3,6
E3	pFZ	24	200	D	
E4	"	25	270	D	
E5	"	25	260	D	
M3	"	71	105	M	
M4	"	73	98	M	
F3	"	222	90	D	
F4	"	238	133	D	
U1	"	1160	107	S	7
U2	"	1160	125	S	7
S2	pP	11	110	M	3
O1	"	32	260	M	3,4
P1	"	50	37	M	1,3
R2	"	250	51	S	1,3

nFZ: n-type float-zoned   nP: n-type pulled   PFZ: p-type float zoned
pP: p-type pulled

D: Dupont   M: Monsanto   S: Semi-elements, Inc.

1. strong injection level effects seen   5. thin (1.4mm) sample
2. axial cut crystal   6. lateral resistivity
3. long time constant traps   gradients
4. large minority carrier trap concentration 7. severe lifetime gradients

† at room temperature

Table 2

Radiation History of Samples Used

Data Set[*]	Total Dose (10⁶ Roentgens)	Data Set[*]	Total Dose (10⁶ Roentgens)
B2-1	.2	I4-1	5
B3-1	.1	I4-2	10
B3-2	.2	L3-1	.2
C1-A1	3	L3-2	.4
C3-1	.1	L5-1	.1
C4-1	.2	L5-2	.2
C4-2	.4	M3-1	2
C4-3	.8	M4-1	1
C4-4A	10	O1-1	2.5
C6-1	.2	O1-2	5
C6-2	.4	P1-1	5
C6-3	.8	P1-2	10
E3-1	4	R1-1	11
E4-1	2	R2-2	20
E4-2	4	S1-1	2
E5-1	2	S1-2	.4
E5-2	20	S1-3	.9
F3-1	2	T4-1	2.5
F3-2	4	T4-2	.5
F3-3	9	T7-1	2.5
F3-4	18	T7-2	.5
F4-1	2.5	U1-1	2.5
H1-1	5	U1-2	5
H2-1	2	U2-1	5
H2-2	4	U2-2	10
I1-1	12		
I1-3	20		

[*]Sample is denoted by first letter and number. Second number denotes number of irradiation.

Table 3

List of Computer Fits

Code	Formula
PFZ-1	$\tau = P_o(A_1,A_2,A_3) = A_1*[1+(\frac{10^3}{T})^{-1.5}*\exp(A_2-11.6*(\frac{10^3}{T})*A_3)]$
PFZ-2	$\tau = P_o(A_1,A_2,A_3)*(10^3/T)^{A_4}$
PFZ-3	$\tau = A_1+(10^3/T)^{A_4-1.5}*\exp(A_2-11.6*(10^3/T)*A_3)$
NFZ-1	$\tau = \frac{P*Q}{P+Q}$, $P = P_o(A_1(P),A_2(P),A_3(P)) = P_o(P)$, $Q = P_o(Q)$
NFZ-2	$\tau = \frac{P*Q}{P+Q}$, $P = P_o(A_1(P),A_2(P),A_3(P))$ $Q = P_o(A_1(Q),A_2(P),A_3(Q))$
NFZ-3	$\tau = \frac{P*Q}{P+Q}$, $P = P_1(A_1(P),A_2(P),A_3(P),1/2)$ $Q = P_1(A_1(Q),A_2(P),A_3(Q),1/2)$

Table 3 (continued)

PP-1	$\tau = P_2(P) = A_1*(1+\exp(A_4-A_5*(10^3/T)$ $+ (10^3/T)*\exp(A_2-11.6*A_3*(10^3/T))$
PP-2	$\tau = \dfrac{P*Q}{P+Q} \quad P = P_o(P), \quad Q = P_2(Q)$
NI-1	$$\tau = \frac{A_1*(n(A_4)+A_2*(10^3/T)^{-1.5}*\exp(47.1-11.6*(10^3/T)*A_3))}{[n(A_4) + p(A_4)]}$$ with $[n(A_4+p(A_4)] = 10^{13}*(A_4{}^2+(10^3/T)^{-3}\exp(38.63-$ $14.04*(10^3/T)))^{1/2}$ and $n(A_4) = (A_4*10^{13}+ [n(A_4)+p(A_4)])/2$

Table 4

Computer Parameters for n-type Float-Zoned Silicon

Data Set	$A_1(P)^a$	$A_2(P)$	$A_3(P)^b$	$A_1{}^a(Q)$	$A_2(Q)$	$A_3(Q)^b$	Fit	$A_{20}{}^c$	$\tau_{po}\phi^d(P)$
B2-1-0	8.33	14.00	.378	.0178	12.58	.089	NFZ-1	13.5	1.66
B3-1-0	23.75	14.22	.40^e	.0207	f	.106	NFZ-2	13.5	2.37
B3-2-0	10.85	14.63	.402	.0094	f	.112	NFZ-2	13.5	2.16
L3-1-0	8.33	16.16	.427	.070	f	.171	NFZ-2	14.95	1.67
L3-1-2	9.72	16.64	.454	.040	f	.18	NFZ-2	14.95	1.94
L3-2-0	4.38	17.96	.487	.030	f	.21	NFZ-2	14.95	1.75
L5-1-0	23.06	14.78	.40	.0016	f	.103	NFZ-2	14.95	2.31
L5-1-2	19.87	15.09	.412	.126	f	.151	NFZ-2	14.95	1.99
L5-2-0	10.0	15.30	.416	.117	15.30	.166	NFZ-1	14.95	2.00
L5-2-0	5.52	15.59	.420	.051	f	.174	NFZ-3	14.95	
C3-1-0	28.35	14.79	.367	.268	f	.130	NFZ-2	15.55	2.84
C4-1-0	12.78	15.23	.383	.037	f	.078	NFZ-2	15.55	2.52
C4-1-2	16.54	16.72	.422	.147	f	.174	NFZ-2	15.55	3.30
C4-2-0	7.07	15.61	.391	.295	15.57	.165	NFZ-1	15.55	2.83
C4-2-0	6.87	15.55	.389				PFZ-1	15.55	2.75
C4-3-0	3.64	15.43	.396	.137	f	.181	NFZ-2	15.55	2.91
C4-4A$_2$-0	12.2	17.07	.461	.053	f	.225	NFZ-2	15.55	1.22
C6-1-0	12.24	15.22	.350				PFZ-1	15.85	2.45
C6-2-0	7.59	16.09	.408				PFZ-1	15.85	3.04
C6-2-3	8.86	17.65	.461				PFZ-1	15.85	3.54
C6-3-0	4.04	16.37	.419				PFZ-1	15.85	3.23

a) τ_{po} for NFZ-1, NFZ-2, PFZ-1 calculations P is for deep level, Q for shallow.

b) Energy level separation from nearest band edge, in eV.

c) $A_{20} = \ln\left[N_c(10^3/T)^{1.5}/Nd'\right]$

d) Product of $A_1(P)$ and net flux in r..

e) Parameter not varied in calculation.

f) $A_2(Q)$ held equal to $A_2(P)$ during calculation

Table 5

Computer Parameters for B-Doped FZ Silicon

Data Set	$A_1(P)^a$	$A_2(P)$	$A_3(P)^b$	$A_4(P)$	$A_1(Q)^a$	$A_2(Q)$	$A_3(Q)^b$	Fit	$A_{20}{}^c$
E4-2-0 E3-1-0	183	10.8^*	$.46^*$		9.71	10.18	.178	NFZ-1	11.4
E5-2-0	32.8	8.4^*	.30*		2.18	9.79	.170	NFZ-1	11.4
E4-2A-2	4.84	14.09	.292					PFZ-1	11.4
M3-1-0	11.52	10.97	.33	-1.0				PFZ-2	12.65
F3-1-0	35.7	11.07	.311					PFZ-1	13.6
F3-2-0	21.1	10.57	.302					PFZ-1	13.6
F3-4-0	5.38	9.06	.250					PFZ-1	13.6
F4-1-0	65.7	13.70	.40					PFZ-1	13.6
F4-A1-0	85.8	10.78	.307					PFZ-1	13.6
F4-A1-A2	106.1	10.83	.306					PFZ-1	13.6
U2-1-0	15.0	12.57	.328	-.5*				PFZ-1	15.4
U2-2-0	5.66	12.44	.318						15.4

a) $A_1 = \tau_{no}$ for PFZ-1, NFZ-1 calculations. $A_1 = \tau_{no}(10^3/T)^{A_4}$ for PFZ-2 fits.

b) Energy level separation from nearest band edge in eV.

c) $A_{20} = \ln[N_V(10^3/T)^{1.5}/N_a{}']$.

d) Combined data sets.

*Parameter held constant during calculation.

Table 6

Computer Parameters for B-Doped Pulled Silicon

Data Set	$A_1(P)$	$A_2(P)$	$A_3(P)^a$	$A_4(P)$	$A_5(P)$	$A_1(Q)$	$A_2(Q)$	$A_3(Q)^a$	Fit	$A_{20}{}^b$
S2-1-0	15.18	10.00	.189						PFZ-1	10.7
S2-1-0	15.11	11.79	.175*	9.52	2.96				PP-1	10.7
S2-2-0	8.34	11.31	.175	10.88	3.50				PP-1	10.7
S2-2-3	3.25	9.97	.167						PFZ-1	10.7
S2-3-0	2.61	10.02	.180						PFZ-1	10.7
01-1-0	15.09	11.06	.164	11.5*	3.46*				PP-1	11.7
01-1-0	13.61	10.09	.186						PFZ-1	11.7
01-2-0	5.93	10.27	.374	12.04	3.16	421	13.0*	.56*	PP-2	11.7
01-2-0	3.60	11.38	.175			2062	12.0*	.45*	NFZ-1	11.7
01-3-0	4.072	10.46	.195						PFZ-1	11.7
P1-1-0	1.107	12.64	.175*	11.5*	3.46*	260	14.0*	.56*	PP-2	12.2
P1-2-0	8.94		.156			187.4	9.2*	.33*	PP-3	12.2

a) Energy level separation from nearest band edge in eV.

b) $A_{20} = \ln[N_V(10^3/T)^{1.5}/N_a']$

*Parameter held constant during calculation.

FIGURE CAPTIONS

Fig. 1. Radiation induced lifetime versus reciprocal temperature in P doped float-zoned (FZ) Si. Curve parameters are given in Table 4. Sample histories and characteristics for all samples are given in Tables 1 and 2. (a) 18 ohm-cm (B) and 68 ohm-cm (L) material. (b) 140 ohm-cm material.

Fig. 2. Lifetime annealing function f (see Eq. (15)) versus temperature of annealing for 10 minute isochronal anneals of P doped FZ Si. The error bars on this and similar figures illustrate the estimated limits of error at selected points.

Fig. 3. Temperature dependence of the defect induced lifetime in annealed P doped FZ Si. Curve parameters are given in Table 4. B3 annealing conditions: 1 hr. at 140°C. C4 annealing conditions: 13 hr. at 145°C followed by 20 min. at 250°C.

Fig. 4. Temperature dependence of the defect induced lifetime in P doped pulled Si. (a) Radiation induced lifetime in 25 ohm-cm (H) and 79 ohm-cm (T4) material. The curves labeled τ, τ_1, and τ_2 relate to the data set H1-1-0, with $\tau^{-1} = \tau_1^{-1} + \tau_2^{-1}$, where τ_1 and τ_2 are PFZ-1 functions whose parameters, as well as those for the T4 curve, are given in the text. (b) 220 ohm-cm material. The I4 curves and the I1-1-3 curve show the radiation induced lifetime for the doses given in Table 2. The curve parameters for the I4 curves are given in the text. The I1-3A-3A2 data set indicates the change of lifetime due to a 6 hr. anneal at 250°C.

Fig. 5. Lifetime annealing function f versus temperature of anneal for 10 minute isochronal anneals in P doped pulled Si. Sample H1 was inadvertently destroyed after the 200°C anneal.

Fig. 6. Temperature dependence of the radiation induced lifetime in B doped FZ Si. Curve parameters are given in Table 5. (a) 225 ohm-cm (F) and 1160 ohm-cm (U) materials. (b) 25 ohm-cm (E) and 72 ohm-cm (M) materials. Curve parameters are given in Table 5.

Fig. 7. Lifetime annealing function f versus temperature of anneal for isochronal anneals of B doped FZ Si. Sample M3 was annealed 20 min. at each temperature, and all others were annealed 10 min. at each temperature.

Fig. 8. Temperature dependence of the defect induced lifetime in annealed B doped FZ Si. Annealing conditions: E4, 20 min. at 200°C; M4, in situ anneal during lifetime measurement with a maximum temperature of 118°C; F4, in situ anneal, maximum temperature 127°C for the F4-A1-0 data set, 135°C for the F4-A1-A2 data set. Curve parameters are given in Table 5.

Fig. 9. Temperature dependence of the radiation induced lifetime in B doped pulled Si. Curve parameters are given in Table 6. (a) 11 ohm-cm (S) and 32 ohm-cm (O) materials. S2-1-0 curves for PFZ-1 and PP-1 fits are indistinguishable. Solid 01-2-0 curve is for NFZ-1 fit, dashed for PP-2 fit. (b) 50 ohm-cm (P) and 250 ohm-cm (R) materials.

Fig. 10. Lifetime annealing function f versus temperature of anneal for 10 minute isochronal anneals in B doped pulled Si.
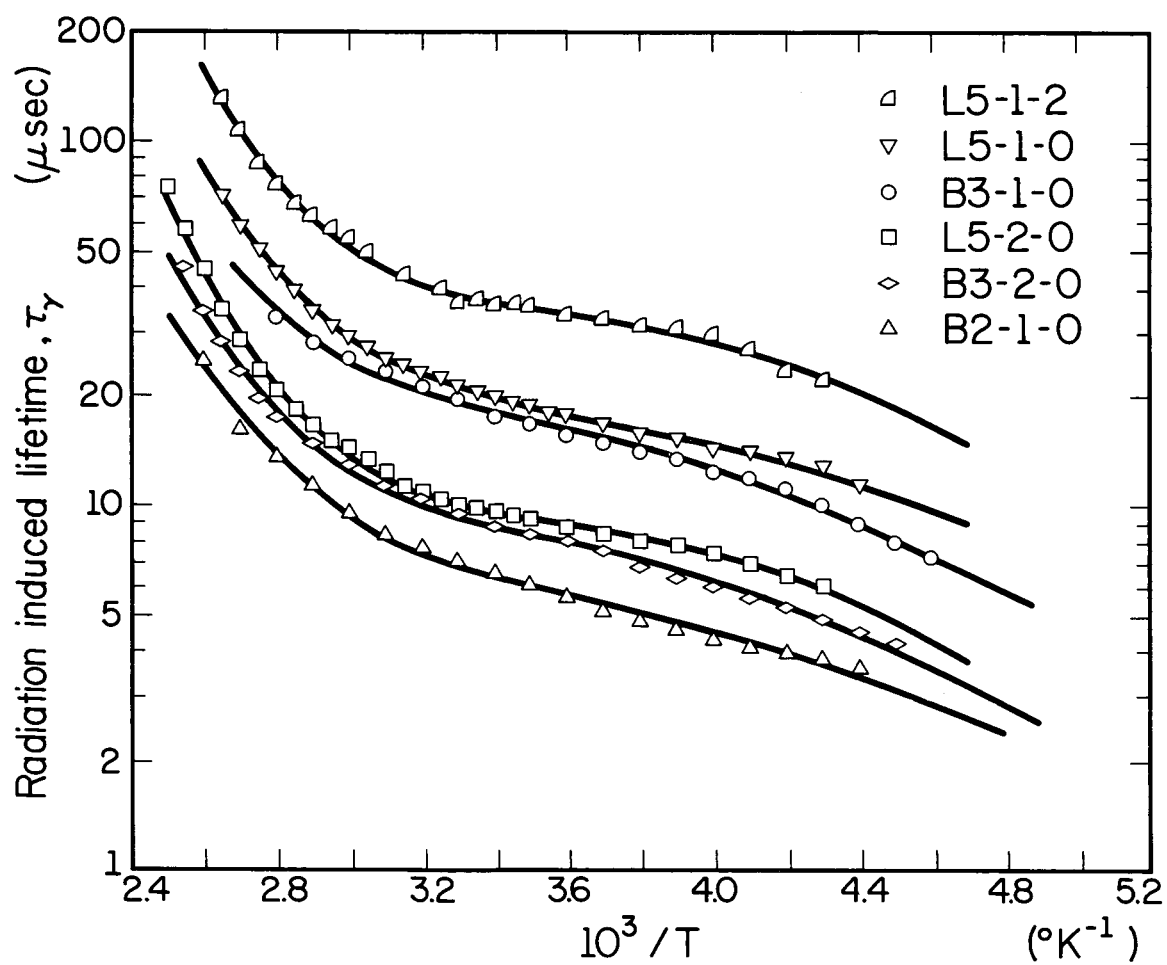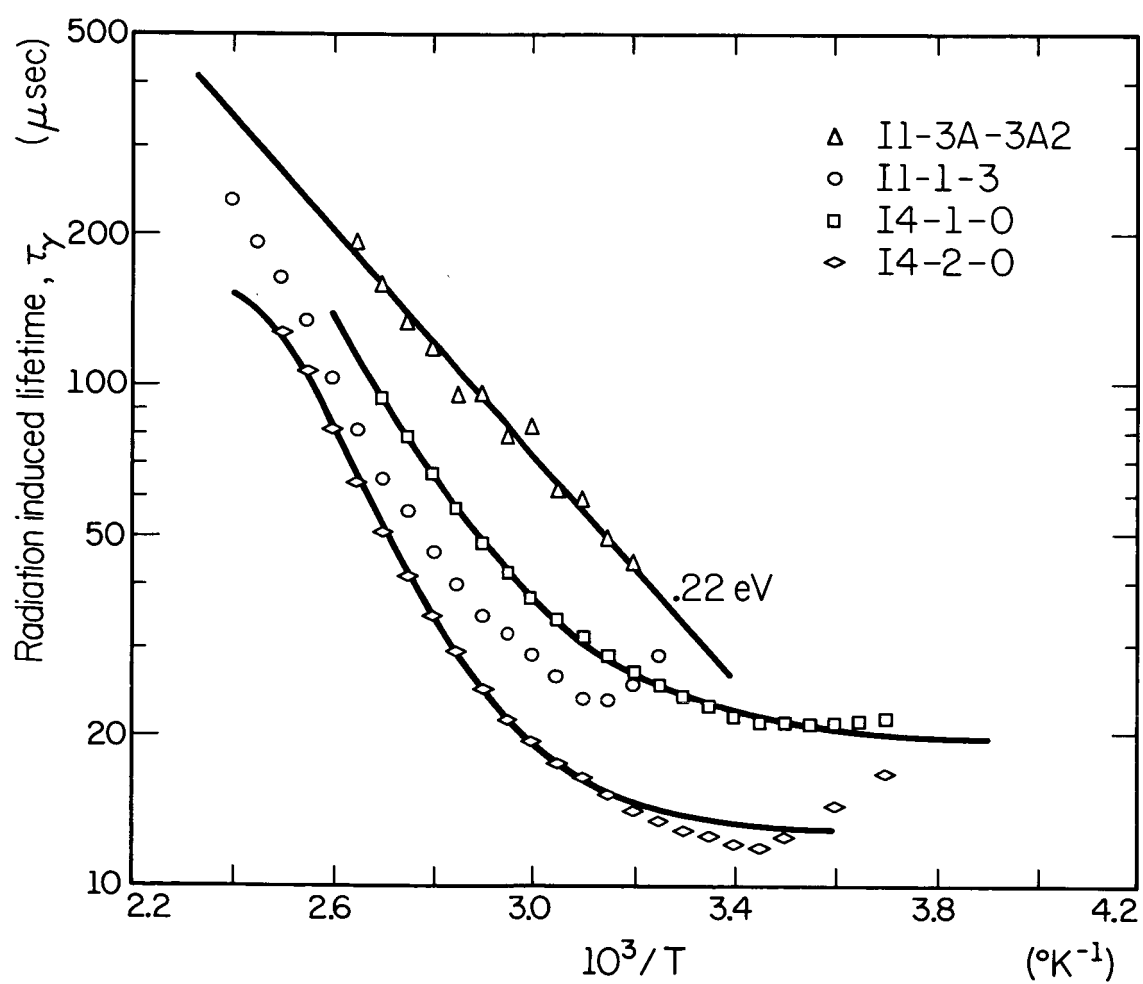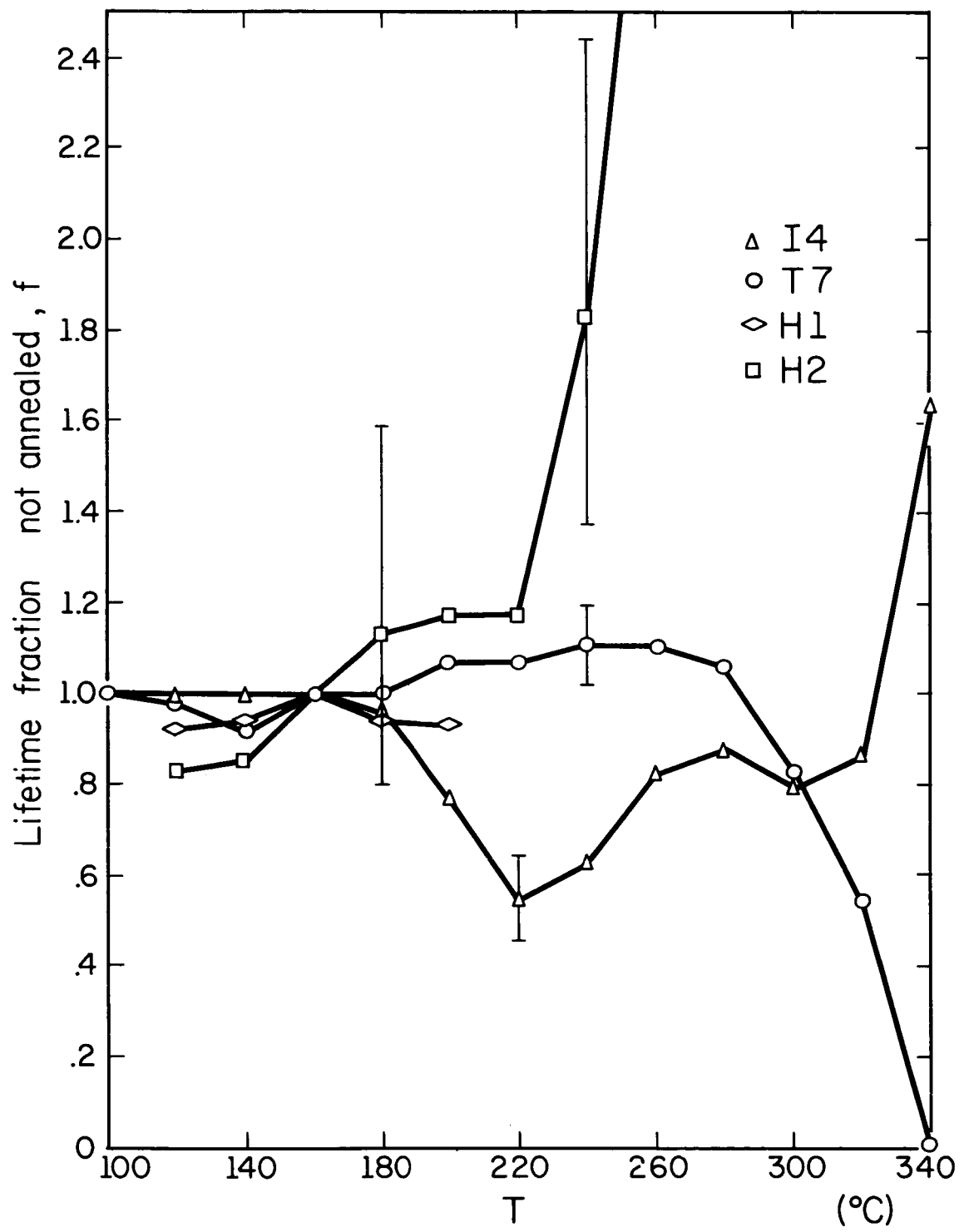
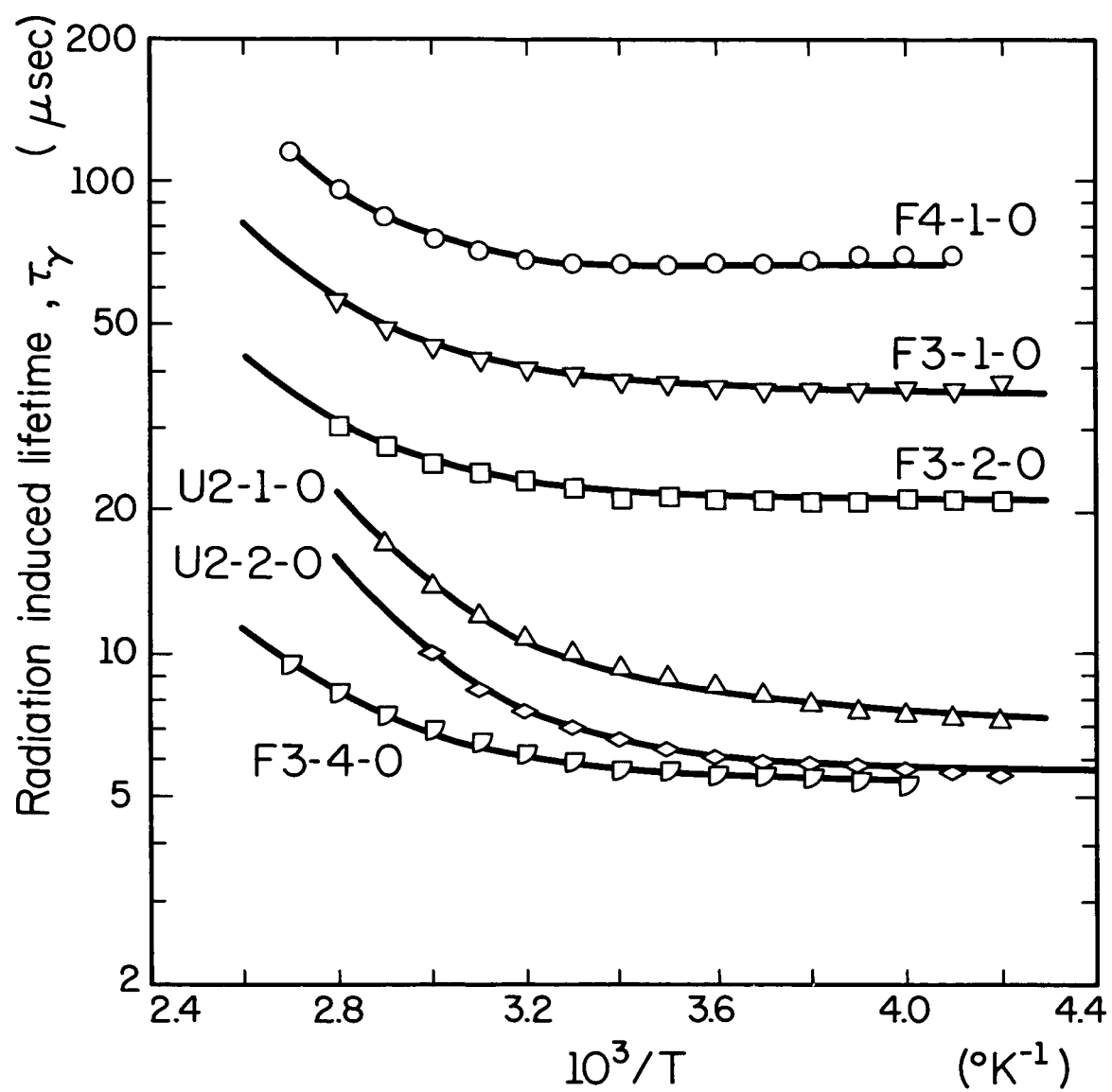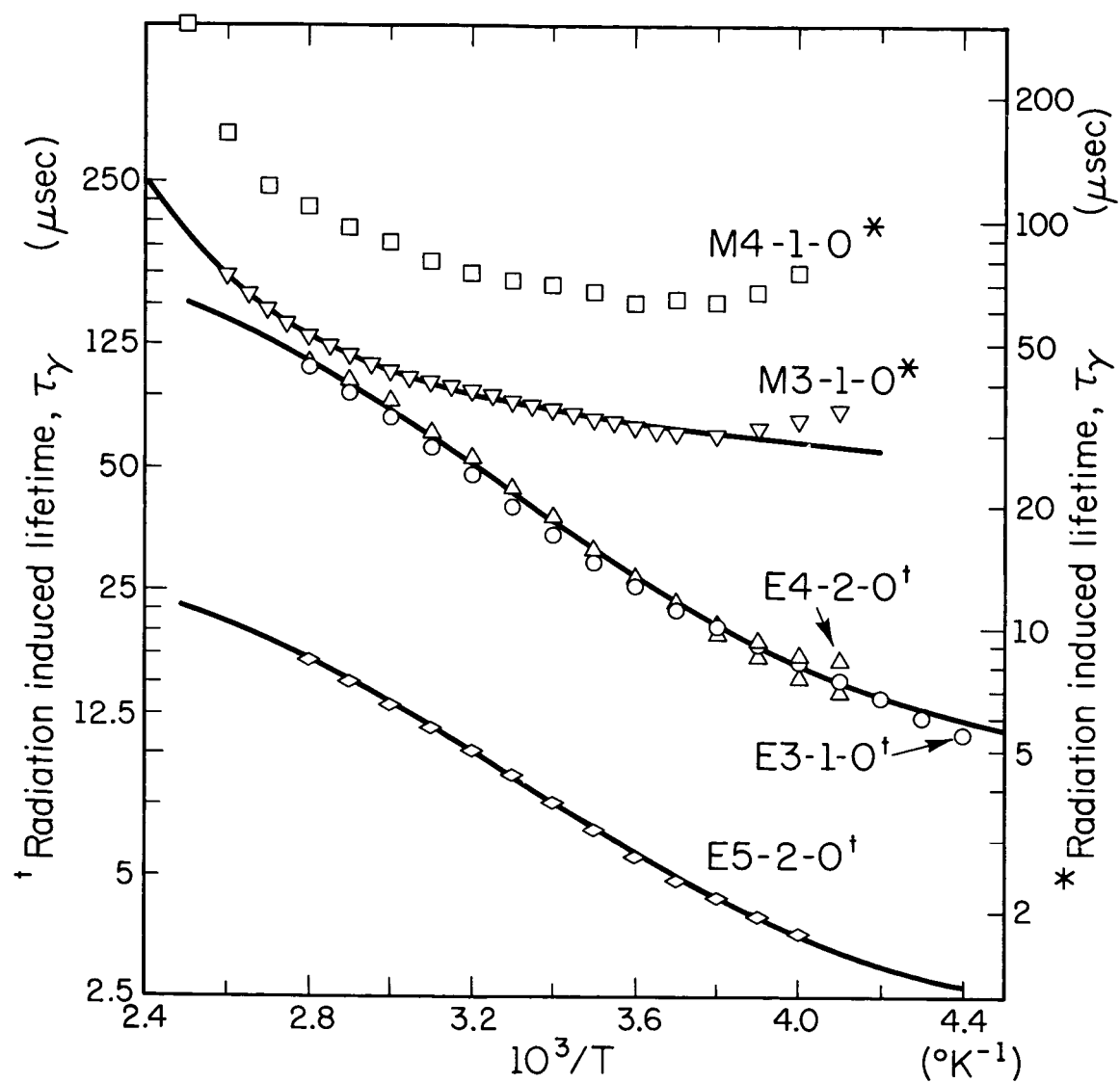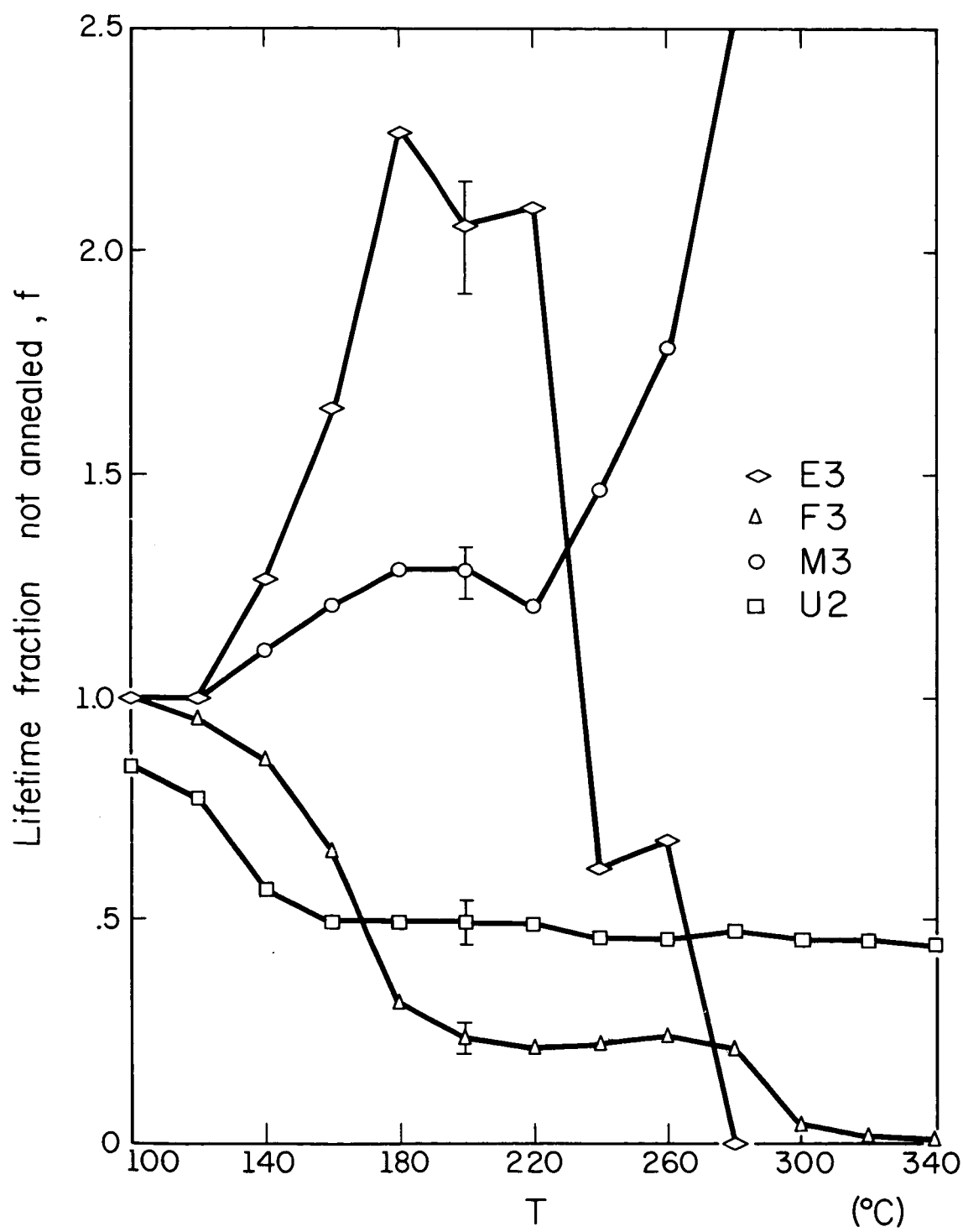Figure 1a
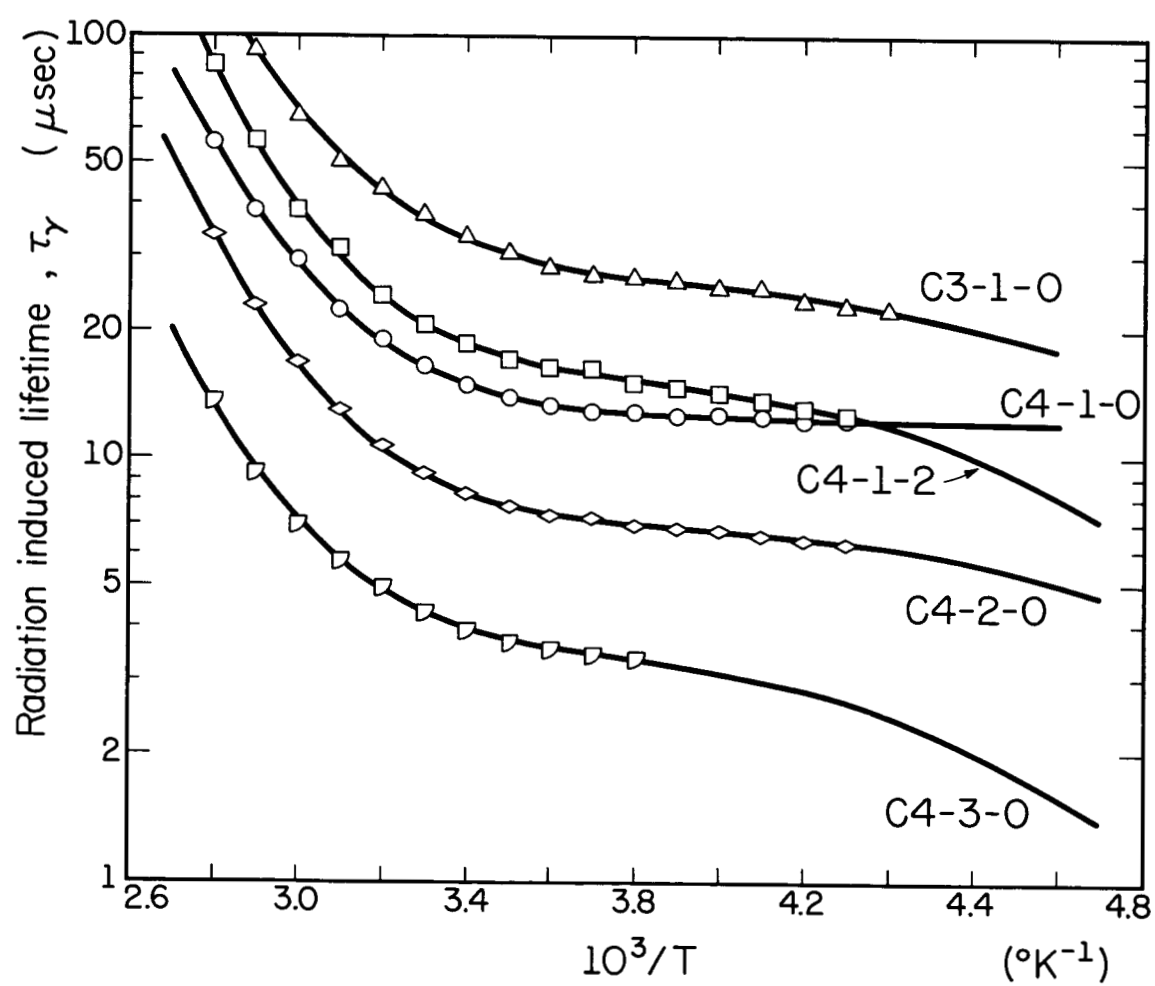
Figure 1b
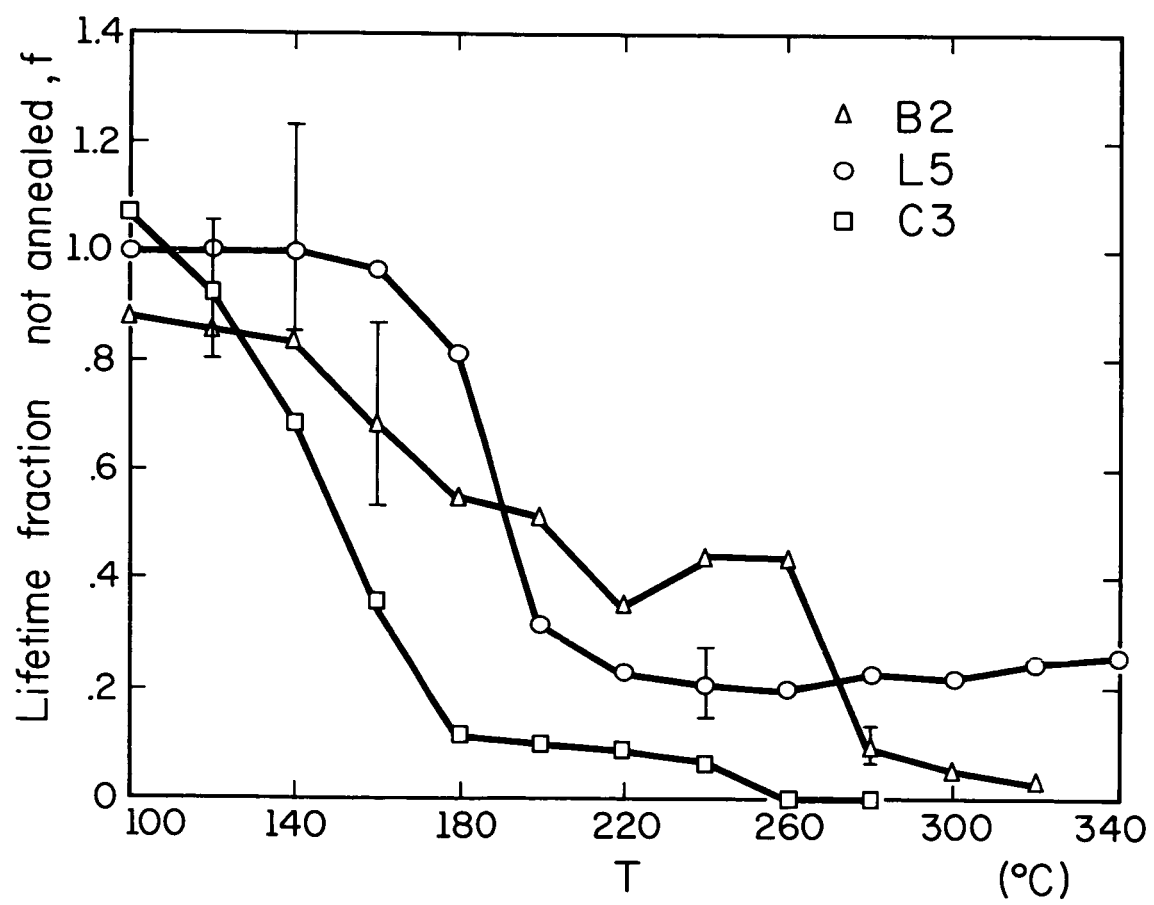
Figure 2
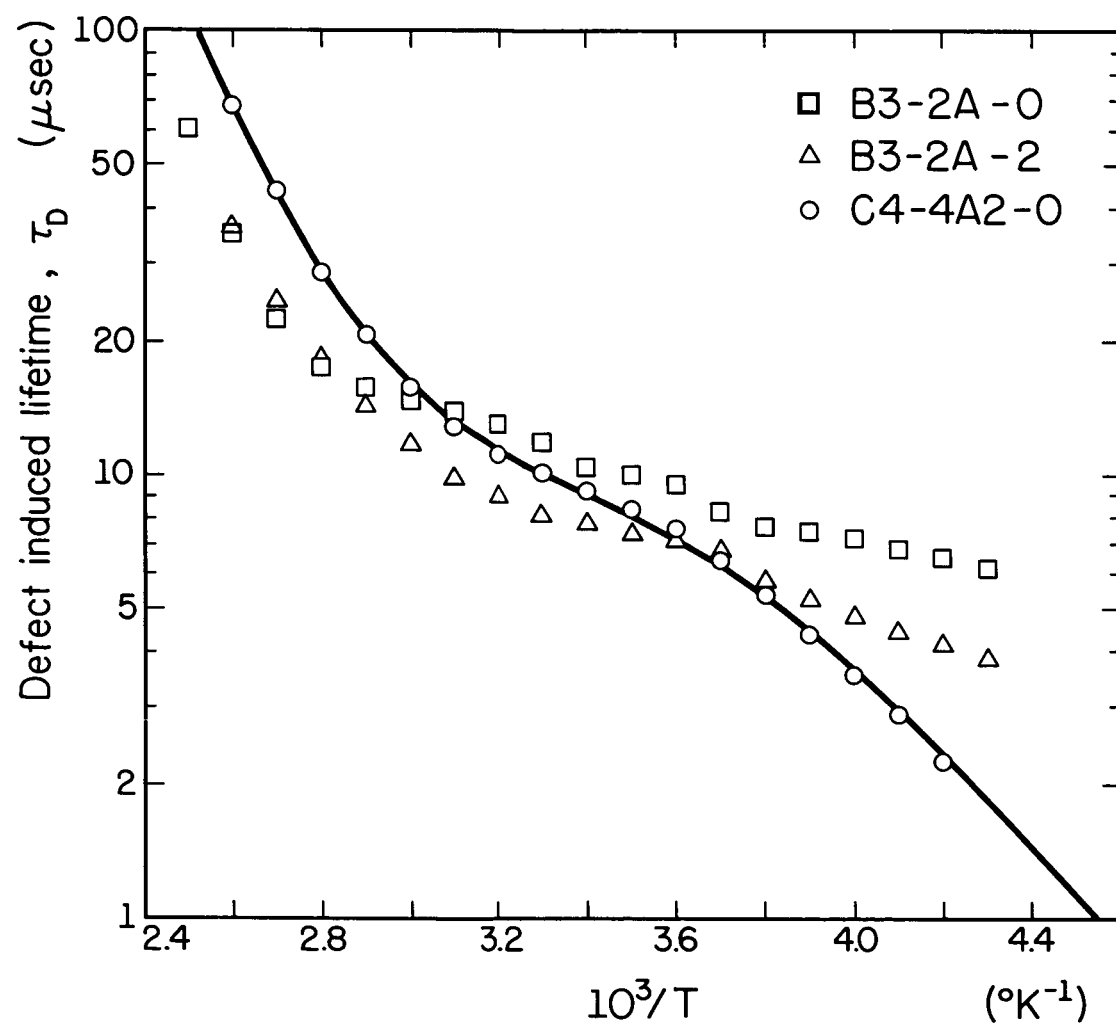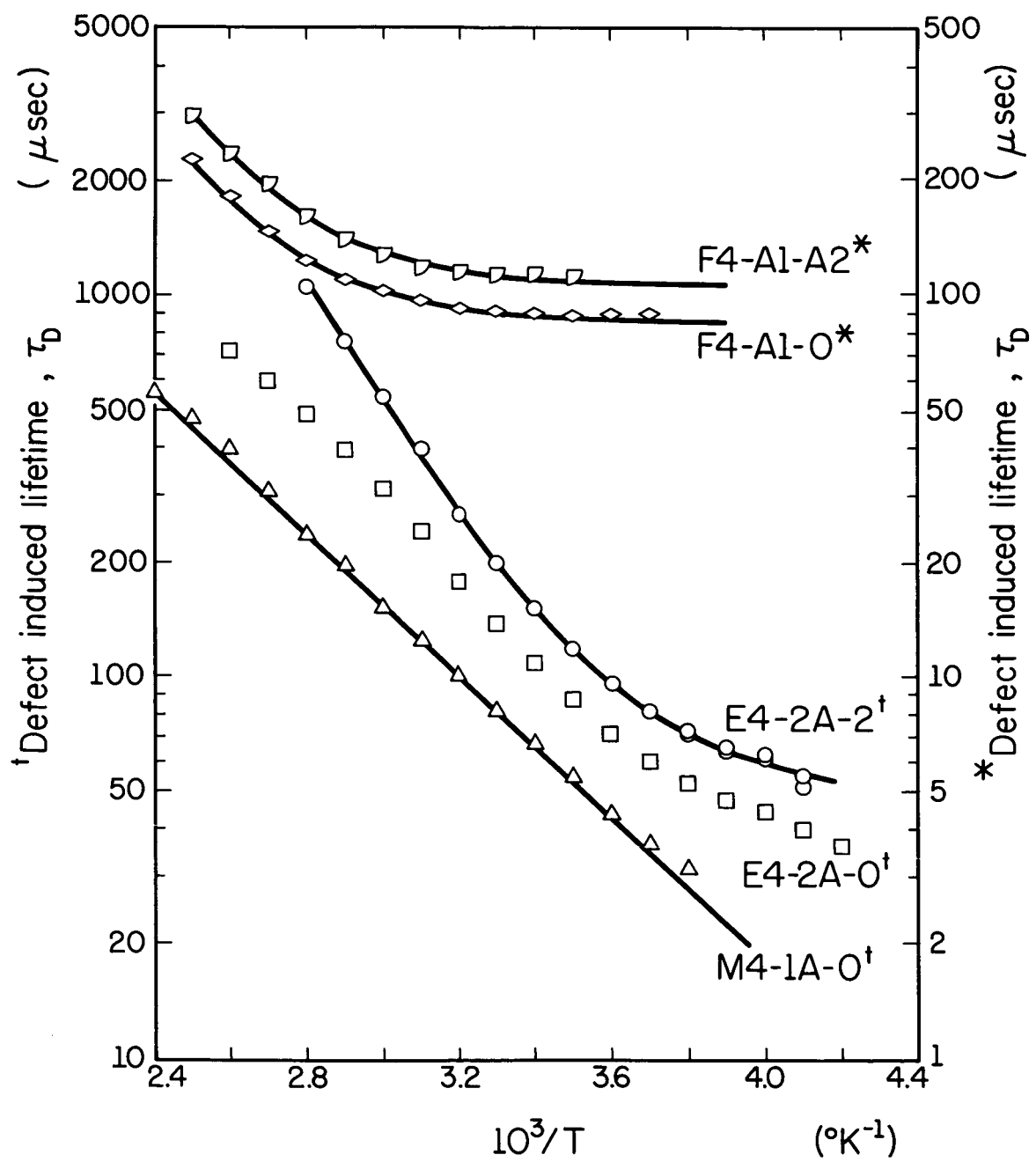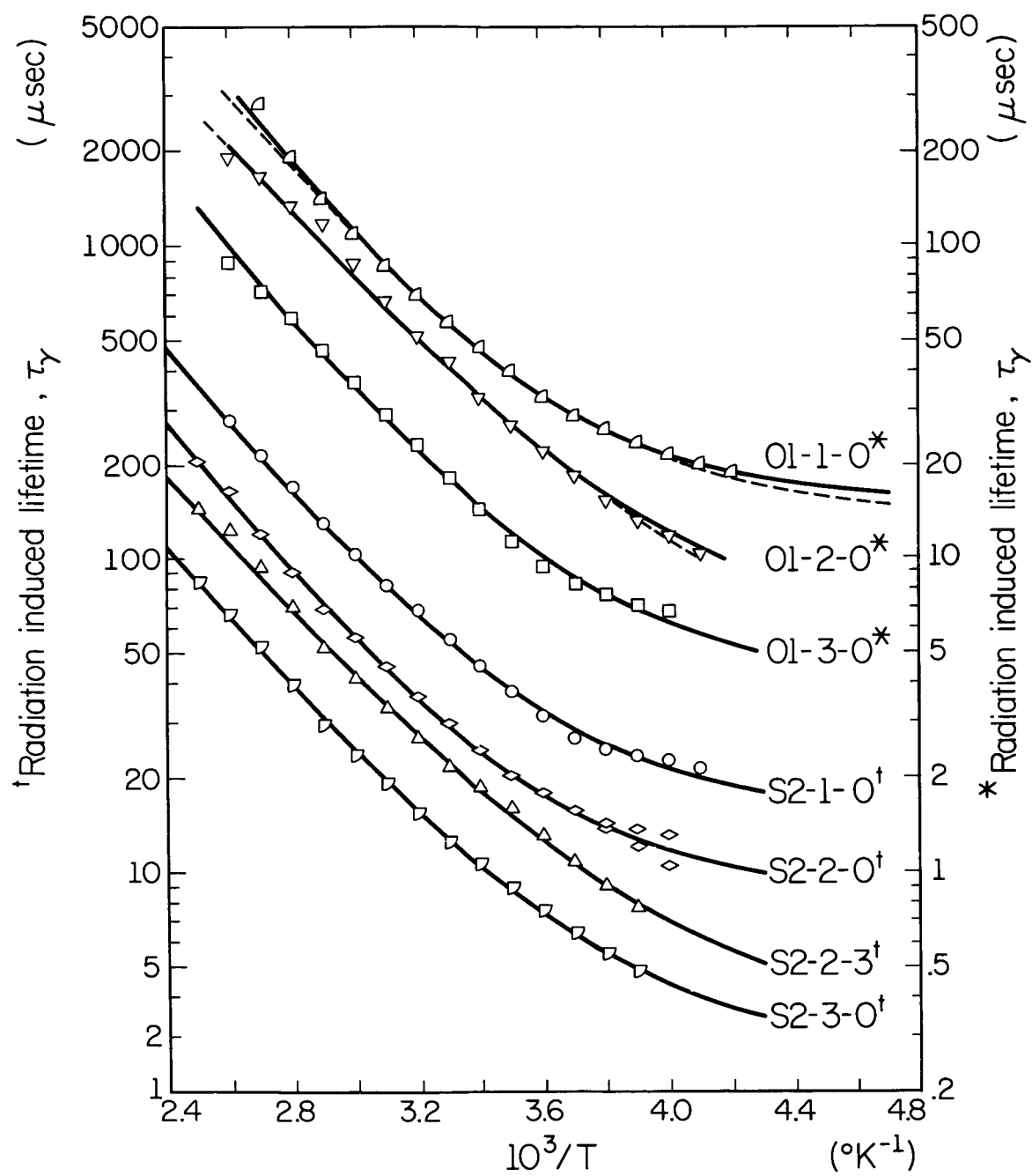
Figure 3
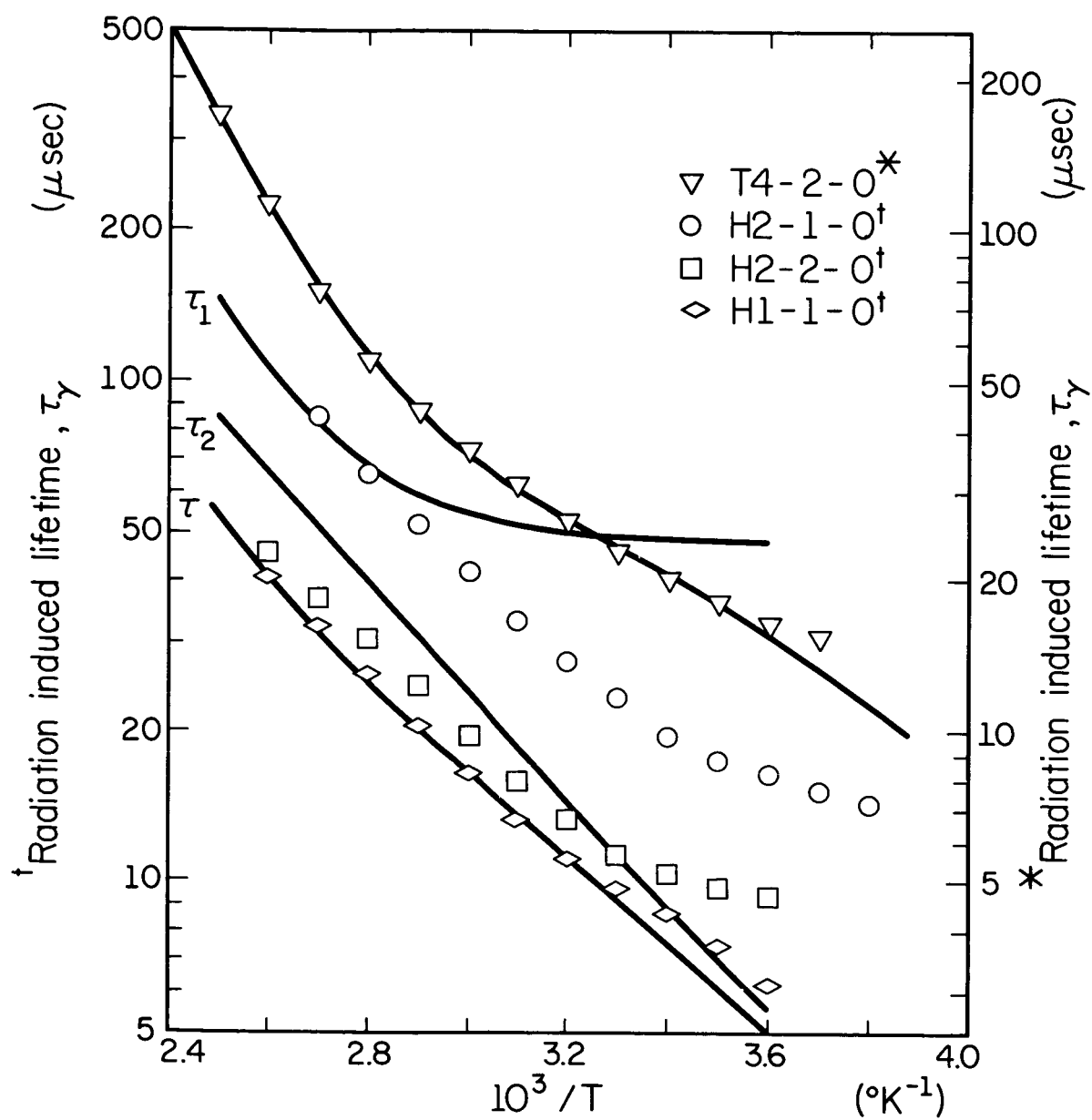
Figure 4a

Figure 4b

Figure 5

Figure 6a

Figure 6b

Figure 7

Figure 8

Figure 9a

Figure 9b

Figure 10